Acceleration and Transition Crossing in Booster

Valeri Lebedev

Accelerator Physics and Technology Seminar
April 26 and May 17, 2016
Fermilab

U.S. DEPARTMENT OF ENERGY

Fermilab

Outline

- Introduction
- Booster Longitudinal impedance
- Beam based measurements
- Data analysis and simulation results
- Gamma-t and Q-t jumps
- Negative mass instability
- Conclusions

Recent History

- Transition crossing has been one of the major bottlenecks limiting Booster intensity
- My involvement to this problem started ~2005 (reported at HB-2006)
  - Change of beam space charge force from repulsion to attraction at transition results in longitudinal quadrupole oscillations ⇒Loss
  - RF voltage jump technique was proposed to suppress it
    - Linear model, V. Lebedev, 2005
    - Simulations, Xi Yang, 2007
  - Empirical tuning of the transition crossing, B. Pellico
    - Formally looks different – in essence it is quite close to the voltage jump technique
    - Has been greatly improved in recent years
  - Both theory and experiment were quite shallow compared to the recent developments considered to be essential for to PIP-II
- PIP-II requires 1.5 times larger intensity within the same emittances
  - Persistent efforts to understand present transition crossing
    - Great improvements both in experiment and simulations

Recent History (1)

Suppression of the bunch self-focusing (actually overfocusing)

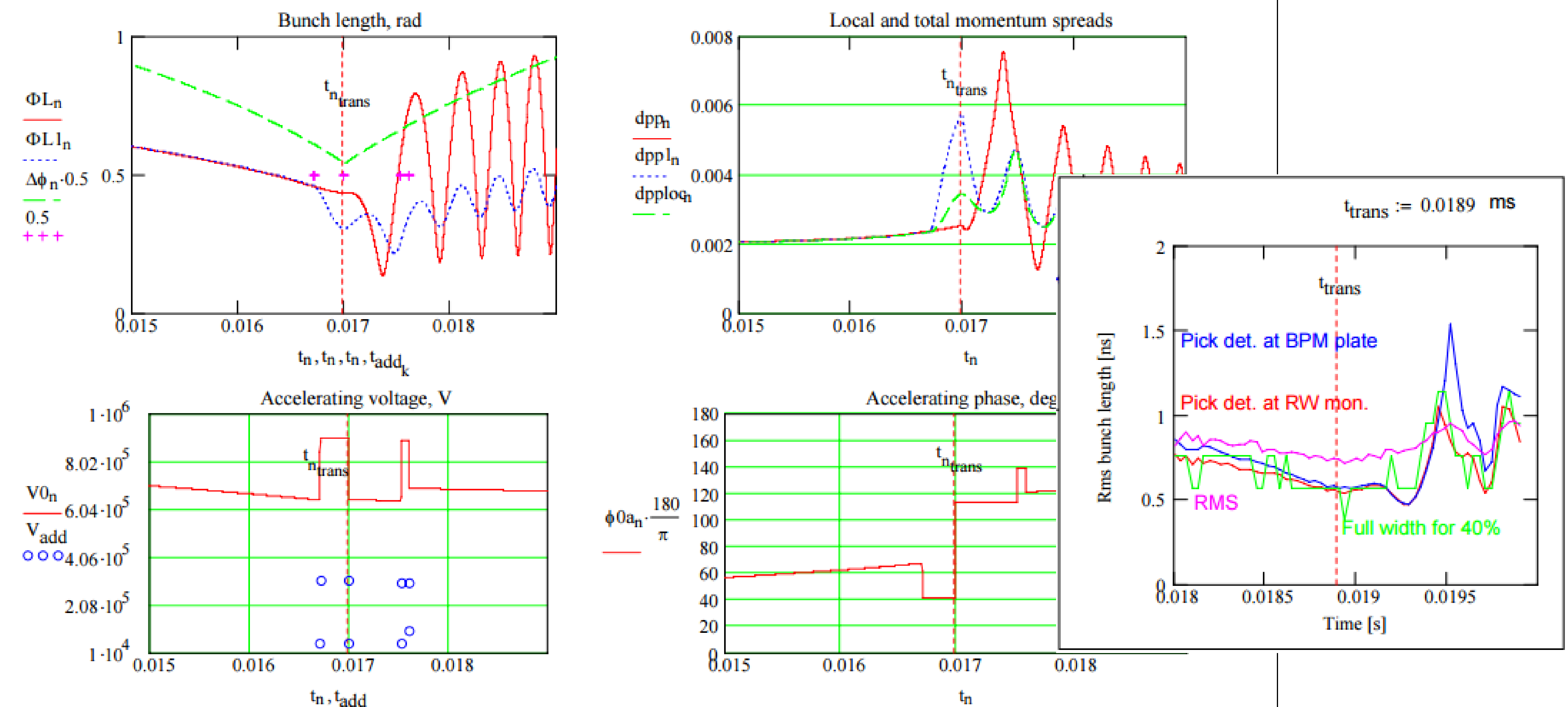

Two pulses. Length and time of the second pulse depends on intensity; for 5e12

- First pulse - duration of ~300 μs just before transition
- Second pulse – duration of ~80 μs, 530 μs after transition

Slide from "Coherent Instabilities in Fermilab Booster" presented at FNAL seminar, June 2006

- Impedance of Booster laminated magnets was completely missed in early considerations – Now we see its significance to the problem.

Acceleration of Low Intensity Beam

- At low intensity
  - Linearized motion equations can be integrated
    ("Acc. Physics" by S. Y. Lee)

$$\begin{cases} \dfrac{d}{dt}\left(\dfrac{\Delta p}{p}\right) = \dfrac{\omega_0 e V_0 \cos(\varphi_{acc})}{2\pi\beta^2\gamma m c^2}\phi\,, \\ \dfrac{d\phi}{dt} = q\omega_0\eta(t)\dfrac{\Delta p}{p}, \quad \eta(t) = \alpha - \dfrac{1}{\gamma^2} = \dfrac{2t}{\gamma_t^{\,3}}\left(\dfrac{d\gamma}{dt}\right) \end{cases}$$

$$\tau_{ad} = \left[\frac{\pi\cdot\beta^2\cdot m\cdot c^2\cdot\gamma_t^{\,4}}{\omega_0^{\,2}\cdot q\cdot e\cdot V_0\cdot\left|\cos(\varphi_{acc})\right|}\cdot\left(\frac{d\gamma}{dt}\right)^{-1}\right]^{\frac{1}{3}}$$

$$\frac{d}{dx}\left[\frac{1}{x}\cdot\left(\frac{d}{dx}\varphi(x)\right)\right] + \varphi(x) = 0 \qquad \text{where:} \quad x = \frac{t}{\tau_{ad}}$$

$$\varphi_1(x) := x\cdot \mathrm{Jn}\left(\frac{2}{3}, \frac{2}{3}\cdot x^{\frac{3}{2}}\right) \qquad \varphi_2(x) := x\cdot \mathrm{Yn}\left(\frac{2}{3}, \frac{2}{3}\cdot x^{\frac{3}{2}}\right)$$

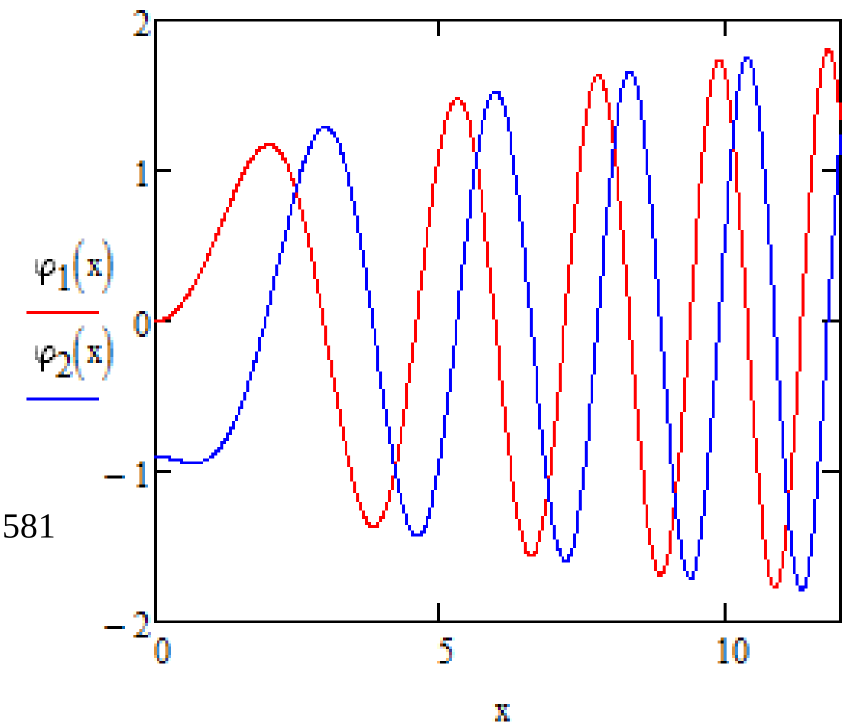

  - No beam loss and emittance growth at transition
  - For FNAL Booster $\tau_{ad} \approx 200\ \mu s$
- Bunch length is getting quite short and weakly depends on machine parameters

$$\sigma_\varphi = \frac{\sqrt[6]{6}}{\pi}\Gamma\left(\frac{2}{3}\right)\frac{q^{2/3}\omega_0^{\,2/3}\sqrt[3]{\tan(\varphi_{acc})}}{(d\gamma/dt)^{1/6}\,\beta_t^{1/3}\gamma_t^{\,2/3}}\sqrt{\frac{\varepsilon_L}{mc^2}}, \qquad \frac{\sqrt[6]{6}}{\pi}\Gamma\left(\frac{2}{3}\right) \approx 0.581$$

where $\varepsilon_L = \pi\sigma_p\sigma_s$ is the total aria in the longit. phase space (L. emit. expressed in eV s)

Acceleration of Low Intensity Beam (2)

At small intensity

- Operation at 20 Hz with 800 MeV (PIP-II) does not require additional RF voltage for the same RF bucket size

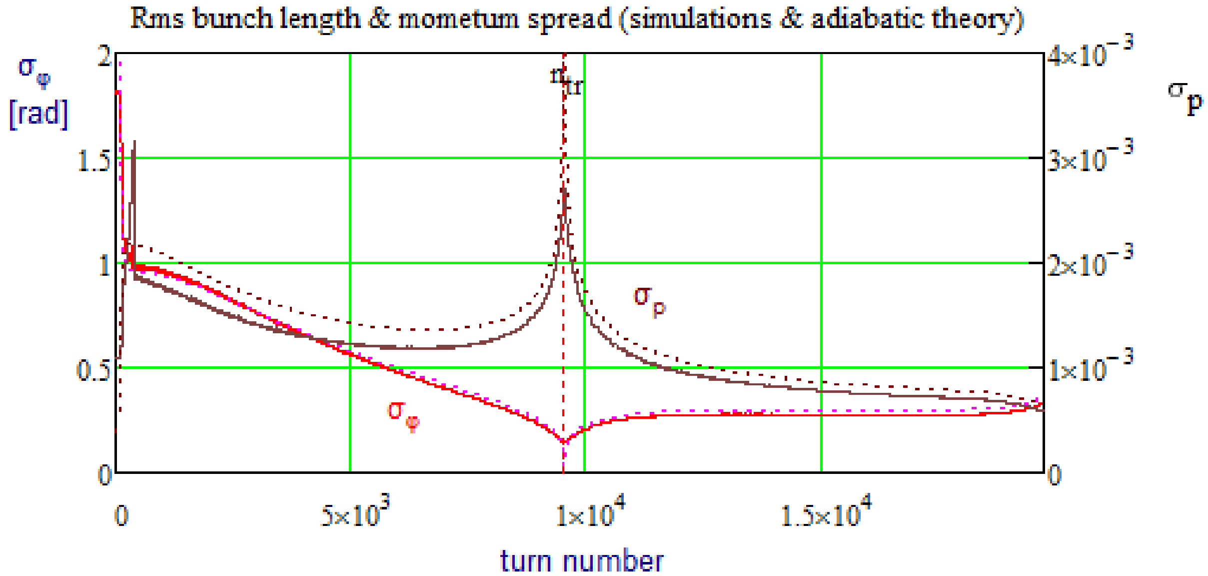

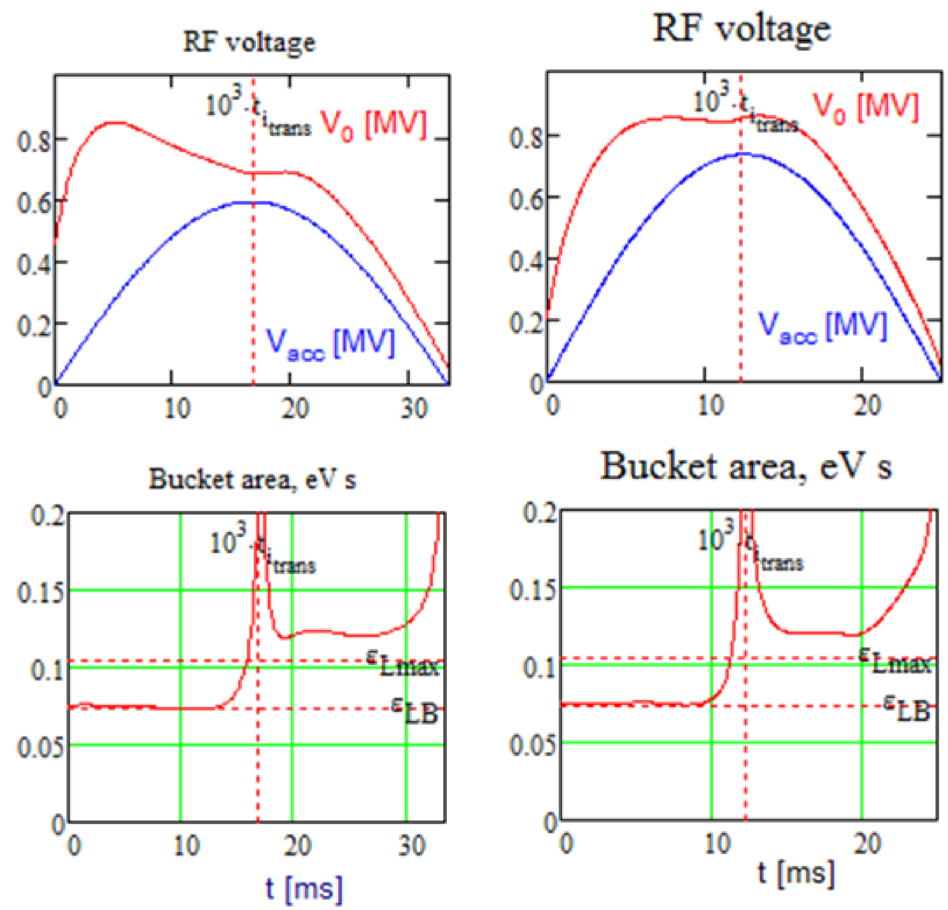

15 Hz 20 Hz

Longitudinal Impedance of the Booster

- Two major contributors to the Booster longitudinal impedance
  - Space charge

$$Z_{\|_{SC}}(\omega) \approx -iZ_0 \frac{\omega}{\beta\gamma^2\omega_0} \ln\left(\frac{r_{chamber}}{1.06\,\sigma_\perp}\right),$$

$$\frac{r_{chamber}}{\sigma_\perp} \geq 2\,, \quad Z_0 \approx 377\,\Omega\,.$$

    - Decreases fast with beam energy but is still important near transition due to very small bunch length
    - Grows linearly with frequency

      Repulsion below transition

      Attraction above transition

      $\Rightarrow$ Quadrupole oscillations
    - $r_{chamber}/\sigma_\perp = 4$ is used in the simulations
  - Wall resistivity
    - Strong beam deceleration at transition where the bunch has the shortest length ($\sigma_t \sim 0.5$ ns, $I_{peak} \sim 7$ A)

Impedance of Booster Laminated Magnets

- Longitudinal impedance of round pipe per unit length

$$Z(\omega) = \frac{Z_0 c}{4\pi}\frac{1+i}{2\pi a \delta_S \sigma} = \frac{Z_0 c}{4\pi}\frac{1+i}{ac}\sqrt{\frac{\mu\omega}{2\pi\sigma}}\ , \quad \delta_S = \frac{c}{\sqrt{2\pi\sigma\omega\mu}}$$

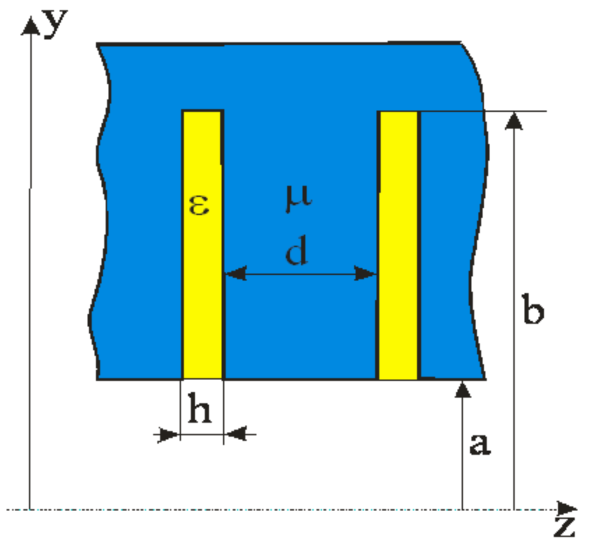

- Laminations greatly amplify impedance
  - (1) $\propto\sqrt{\mu}$, (2) longer current path
  - Impedance of flat chamber per unit length [1]

$$Z_{\|_{LM}}(\omega) = iZ_0\frac{\omega}{2\pi c}\int_0^\infty \frac{F_L(\xi)}{1+F_L(\xi)\tanh\xi}\frac{d\xi}{\xi\cosh^2\xi}$$

where:

$$F_L(\xi) = \frac{h}{d+h}\frac{\xi}{k_y(\xi)}\left(1+(1-i)\frac{\mu\delta_S}{h}\right)\tan\left(k_y(\xi)\left(\frac{b}{a}-1\right)\right),$$

$$k_y(\xi) = \sqrt{\frac{\varepsilon\omega^2 a^2}{c^2}\left(1+(1-i)\frac{\mu\delta_S}{h}\right)-\xi^2}\ ,$$

- The impedance model is expected work well in a frequency range of 0.1 MHz – 1 GHz.
- It takes into account all important details but actual dipoles do not have well-known parameters: *h*? (Packing factor), ε?, μ?

[1] "Accelerator Physics at the Tevatron Collider", editors V. Lebedev and V. Shiltsev

Permeability of Soft Steel

- At high frequencies the skin depth is smaller or comparable to the magnetic domain size
- Measurements @FNAL in summer of 2011

Proceedings of IPAC2012, New Orleans, Louisiana, USA WEPPD079

MEASUREMENTS OF MAGNETIC PERMEABILITY OF SOFT STEEL AT HIGH FREQUENCIES *

Yu. Tokpanov#, V. Lebedev, W. Pellico, Fermilab, Batavia, IL 60510, USA

- Wave propagation in transmission line made from soft steel and located in external magnetic field

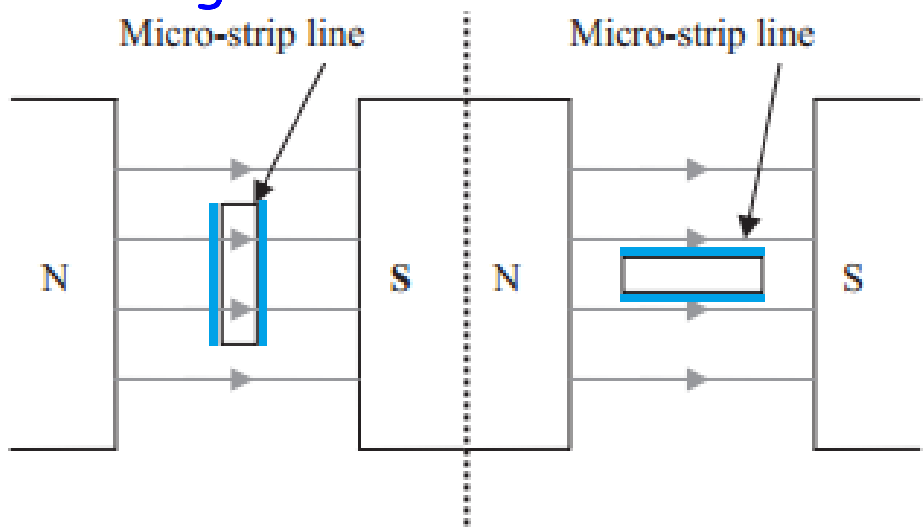

Figure 1: Schematics of the experiment with steel in DC magnet. The normal orientation is represented on the left, and the parallel one on the right.

Permeability of Soft Steel: Results [Tokpanov, IPAC2012]

- μ used in the simulations

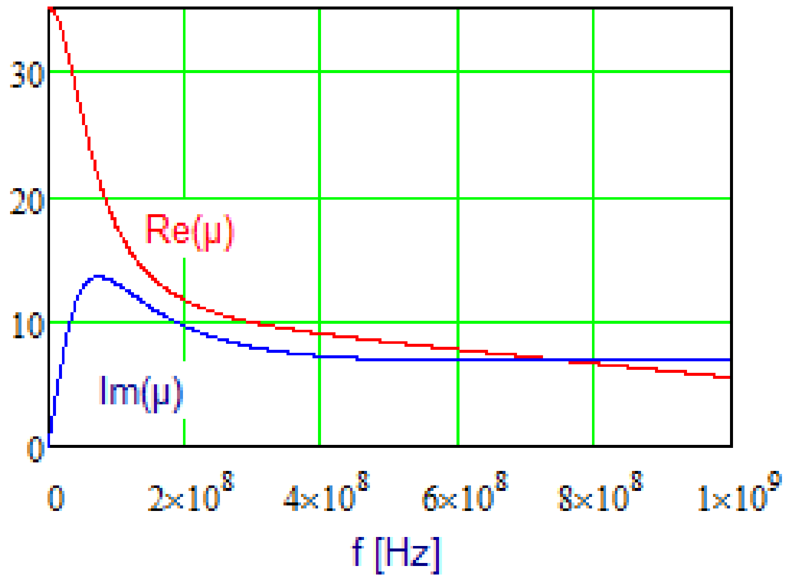

$$\mu(\omega) = \frac{26}{1 + i\omega/\omega_1} + \frac{9}{(1 + i\omega/\omega_2)(1 + i\omega/\omega_3)},$$

$$\omega_1/2\pi = 70\ \text{MHz},\ \omega_2/2\pi = 1.5\ \text{GHz},\ \omega_3/2\pi = 6\ \text{GHz},$$

- Both real and imaginary parts are taken into account
  - ♦ Steel conductivity at high frequencies is assumed to be the same as for DC

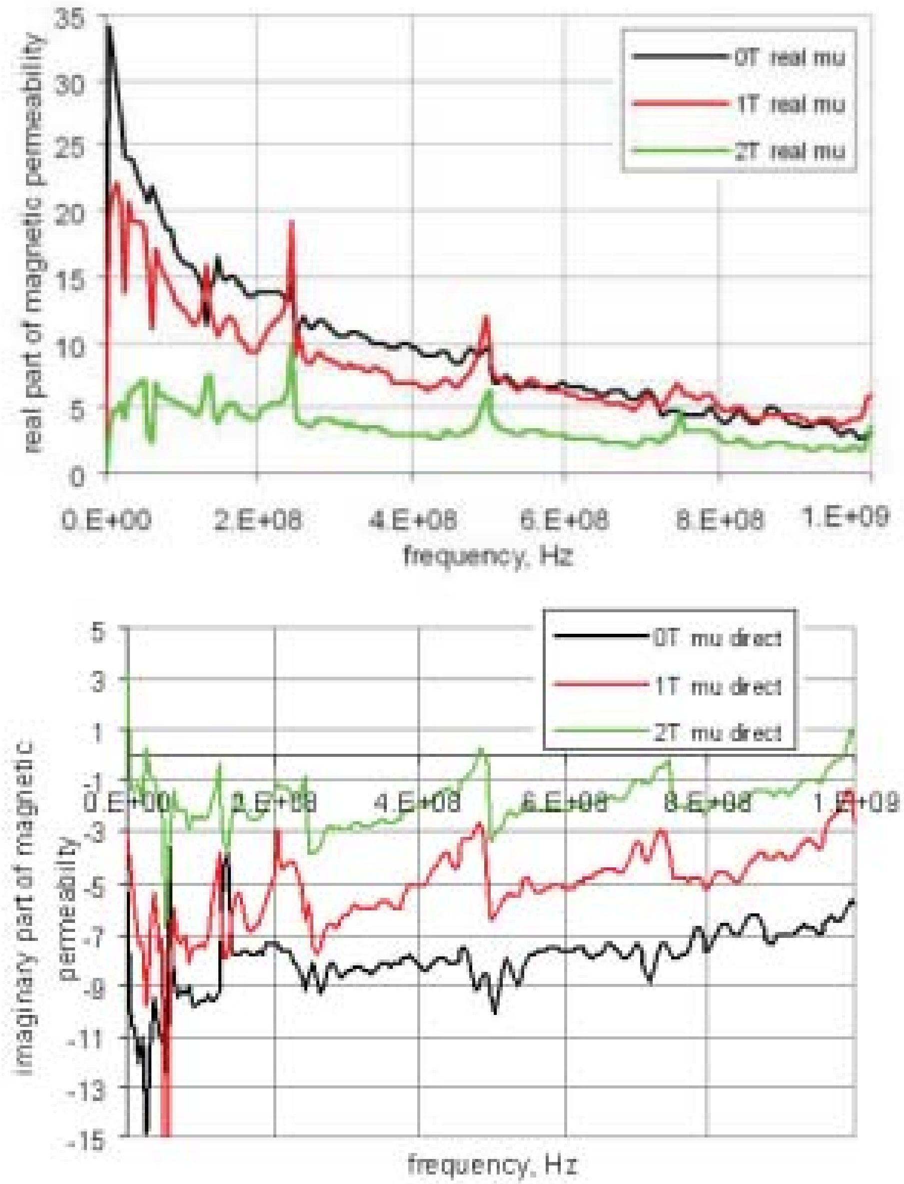

Figure 3: Dependence of magnetic permeability of steel on frequency for different magnetic fields for the case of magnetic field normal to the strip plane.

Parameters for the Impedance Calculation

- Initially *h* was taken from the packing factor 98.5% (Booster design report) and insulating layer thickness: *h*=10+2*10 μm
- ε: epoxy & insulating oxide layer on steel (ε~2 - 3)
- h and ε are updated based on beam measurements
- F dipole has smaller gap and larger impedance

Dipole type	F	D	
Dipole length	2.89		m
Number of dipoles	48	48	cm
Half-gap, *a*	2.1	2.9	cm
Lamina half-height, *b*	15.2		cm
Lamina thickness, *d*	0.64		mm
Dielectric crack width, *h*	45		μm
Conductivity, σ	$2.07\cdot10^{16}$ ($2.3\cdot10^{6}\ \Omega^{-1}\ m^{-1}$)		s^{-1}
Dielectric permittivity, ε	2.5		

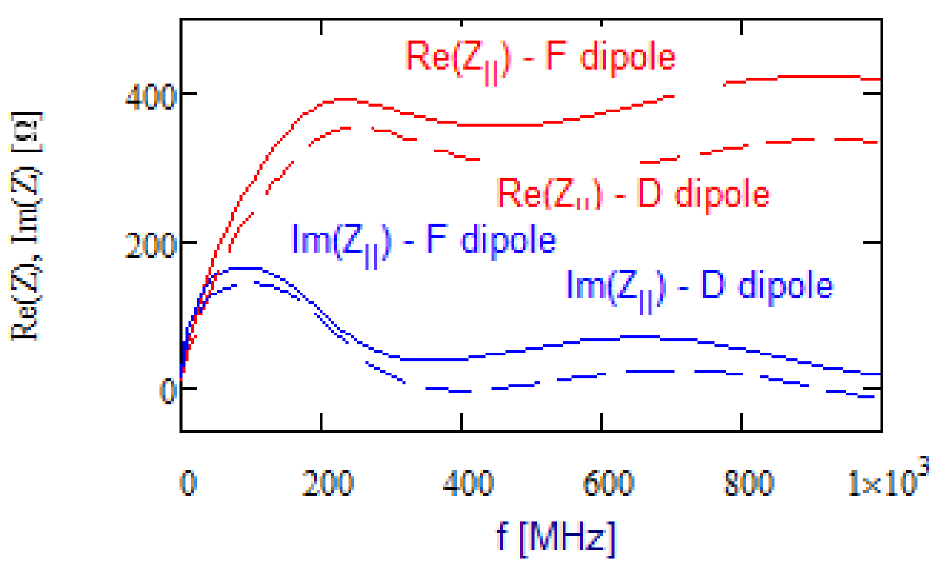

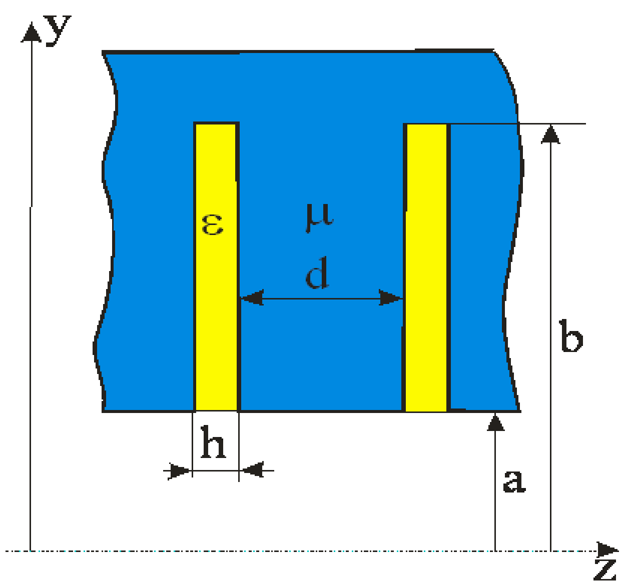

Dependence of longitudinal impedance of Booster dipole on the frequency computed for F and D dipoles.

Stretched Wire Measurements of Longitudinal Impedance of Booster Laminated Dipoles

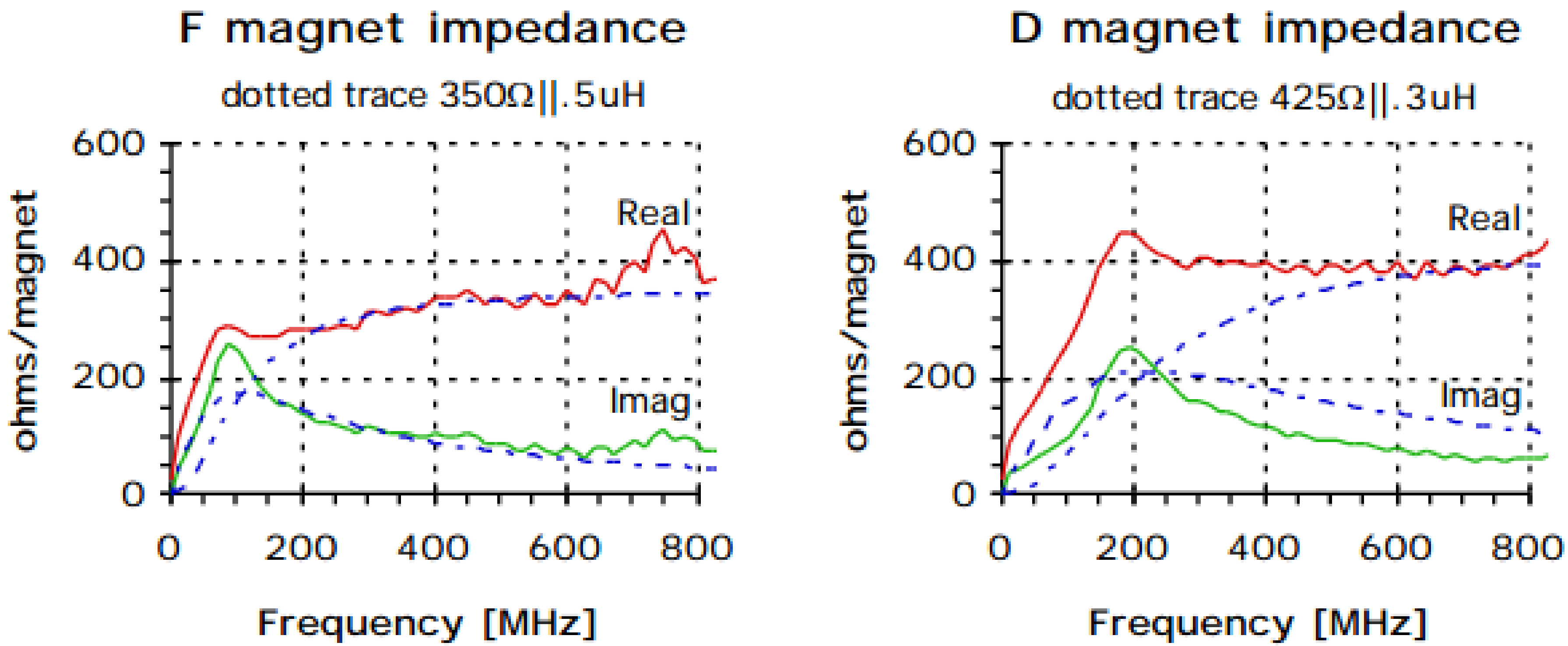

Taken from J. Crisp and B. Fellenz, "Fermilab-TM-2145, March 22, 2001.

- Decent coincidence with the impedance estimate
  - However F magnet impedance ~30% lower than for D-magnet instead of being 10% higher
    - ⇒ We should expect that each dipole has its unique impedance!
    - ⇒ Measurements of total impedance are required
- Expected decelerating voltage = (7.5 A)*(300 Ω)*(48 dipoles)≈**100 kV**

Total Longitudinal Impedance of the Booster

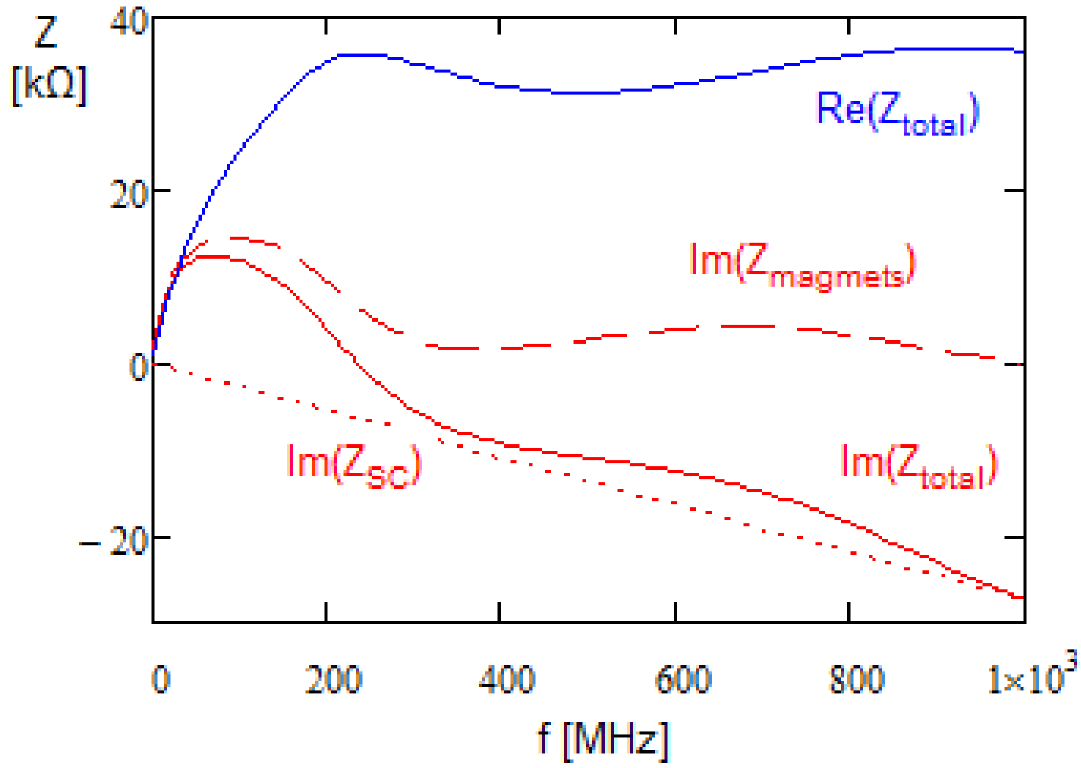

Total longitudinal impedance of the Booster at transition. The impedance value was tuned to the beam-based measurements

- Imaginary part of the space charge impedance is partially compensated by the resistive wall impedance of dipoles
  - At transition the bunch spectrum is extended to 300 – 500 MHz
- Note that wire measurements have noticeably larger imaginary part of the impedance
  - It is not accounted in the below simulations

Beam Based Measurements of the Long. Impedance

- Direct measurements of Z(ω) requires a continues beam
  - Continues beam does not look readily available even at injection energy
  - It is impossible near or at transition
    - μ(B) can make significant correction
- Shift of acceleration phase with bunch intensity allows us to check if the considered above model and wire measurements are applicable
  - Minor adjustments are used for the final tune of the impedance model
    - They do not change significantly the shape of the impedance curve
- ϕ_{accel} is obtained from comparison of
  - RF phase (coming from RFSUM) &
  - Bunch arrival time (coming from RW monitor)

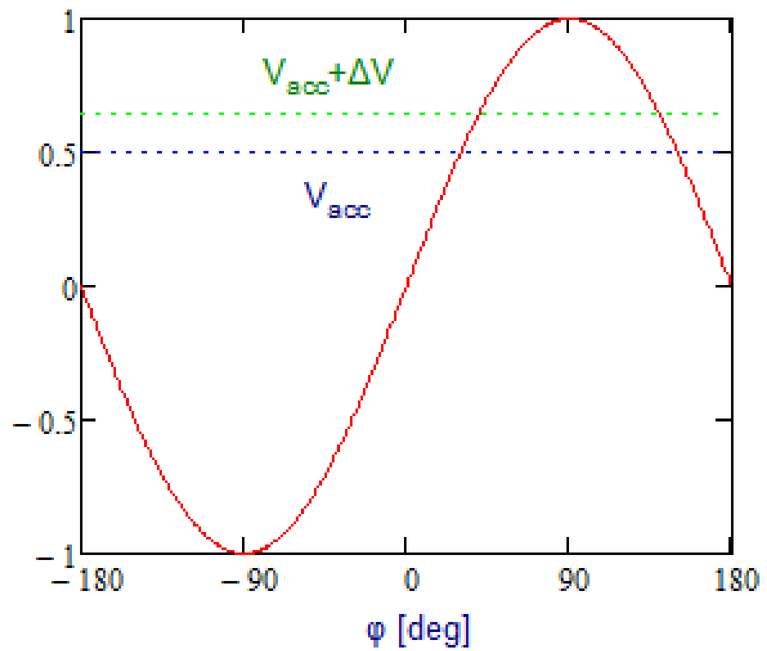

Booster Transition Crossing Studies

- Present transition-X is quiet sophisticated and well-tuned. It effectively suppresses quad-oscillations introduced by the crossing.
- Optimization of transition-X at PIP-II intensity requires good modeling of Booster acceleration and its long. impedance
- 4 sets of measurements
  - Jan, July & Nov /2015
  - Jan/2016)
- Usefulness of data was improved with time
- The last set of measurement is mostly useful and it will be only discussed
  - Data analysis of July'15 data are in PIP-II.doc.db
  - Out of 2 Booster RW monitors the RW monitor with better time resolution was used
- Data are taken at injection and transition
  - Bunch intensities: 4, 8, 12 & 15 turns (2 data sets @ each measurement)
  - 4.8 ms are acquired for each data set
  - Only first 3.6 ms out of 4.8 were used in the analysis due to limitation of data analysis software

Data Acquisition and Preliminary Data Analysis

- RF sum + RWM + Rpos (0.8 ns sampling time, $4.5 \cdot 10^6$ points)

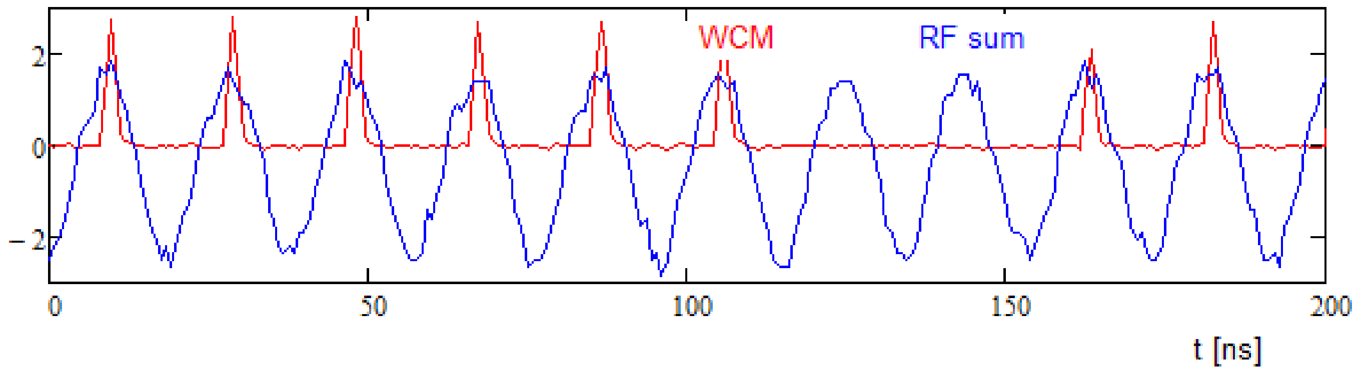

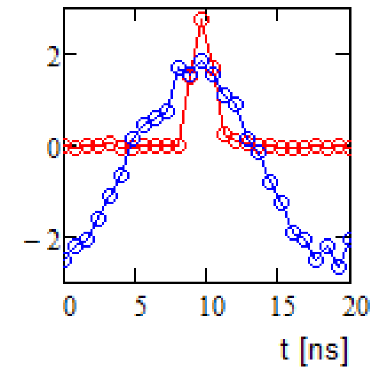

- Needed to have sufficiently long measurements (>3.5 ms) => only few points on bunch length for transition-crossing data
- Data analysis
  - ♦ Fitting RF signal for each period of sinusoid yields
    - ⇒ (1) RF voltage & (2) zero crossing time
      - o RF frequency is computed from zero crossing time
  - ♦ Fitting WCM signal to a Gaussian pulses yields for each period
    - ⇒ (1) Bunch arrival time, (2) Peak height & (3) Peak width
      - o DC offset is not used
      - o Bunch frequency can be computed from Bunch arrival time
  - ♦ Time difference between RF zero crossing and corresponding bunch arrival time yields the relative accelerating phase
    - • correction for cable length difference has to be additionally accounted

Measurements and Corrections for φ_{acc}

- Good reproducibility for 2 sets at each intensity
  - "Transition RF swing" shifts up to 18 turns
  - Both voltage and phase reproduce well
- There is large phase shifts with energy due to difference in cable lengths

$$\delta\varphi = \left(\omega(t) - \omega(t_0)\right)\Delta T$$

  - Injection data more sensitive to this effect due to larger chance in RF frequency,

Δt=1.549 μs

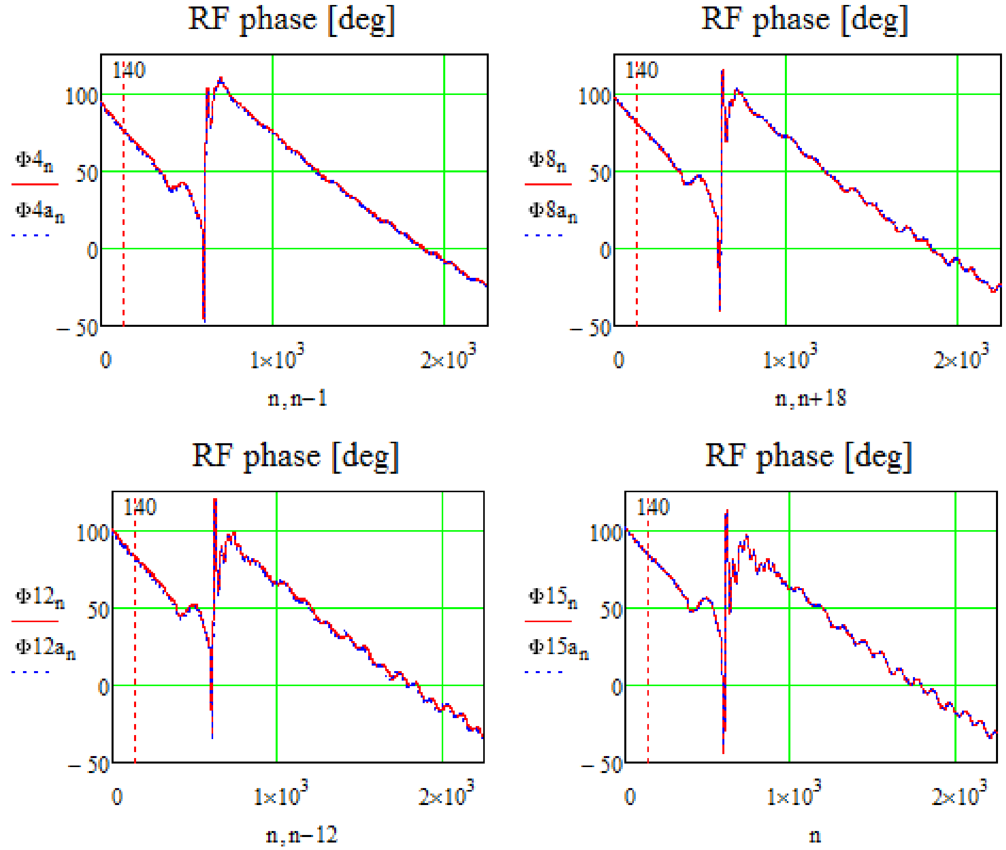

Accelerating phase at transition

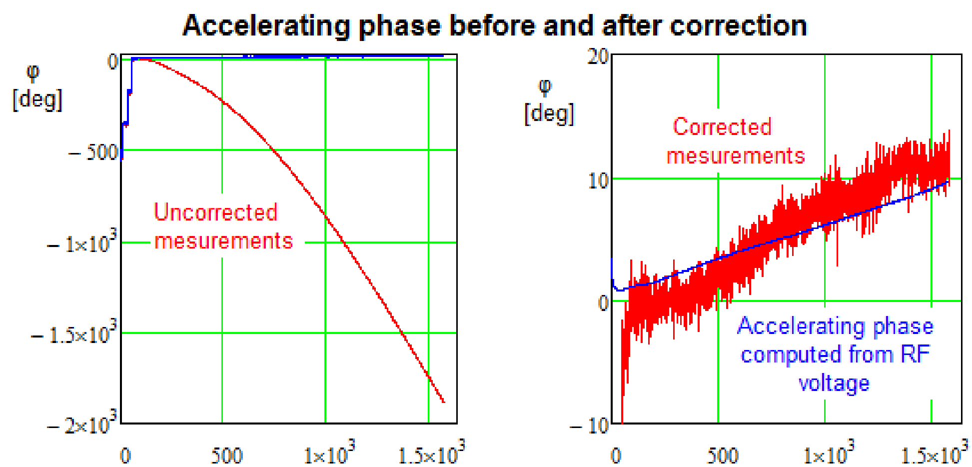

Accelerating phase at injection

Accelerating Phase Shift with Beam Intensity

- The accelerating phase is shifted with intensity close to expectations
- A decrease of RF voltage with intensity increases the resulting shift by ~25%
- Smaller shift after transition is related to larger value of RF voltage after transition

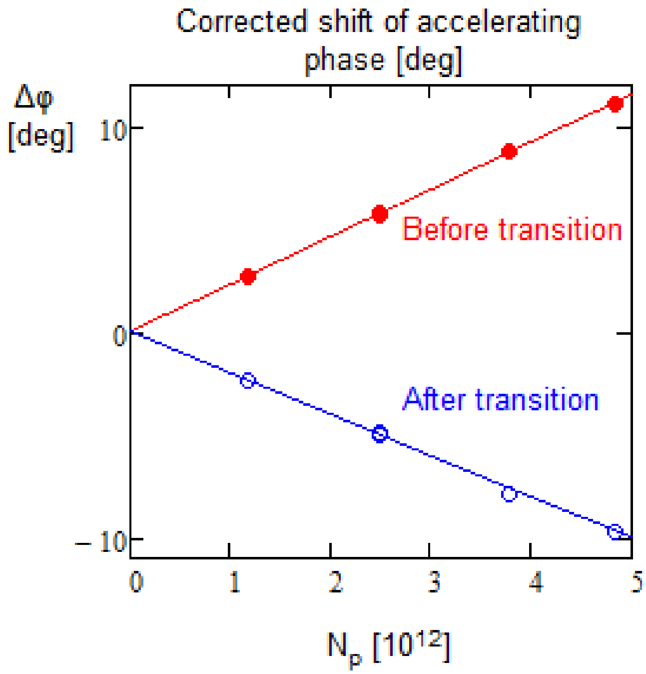

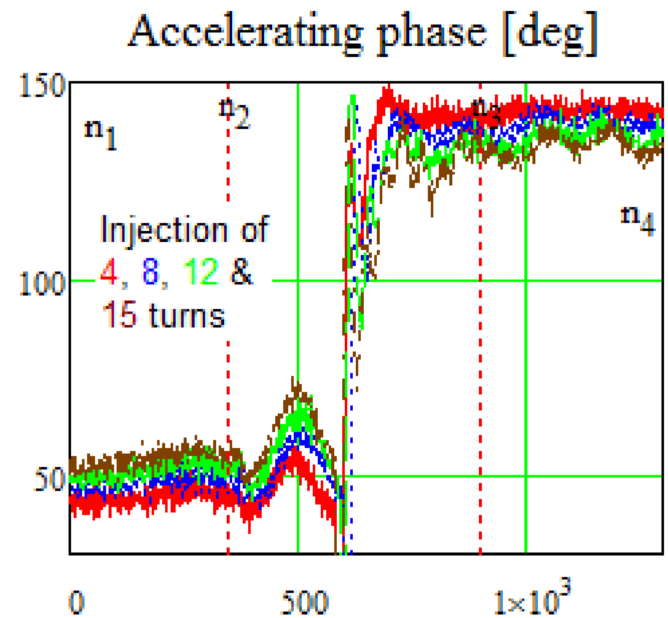

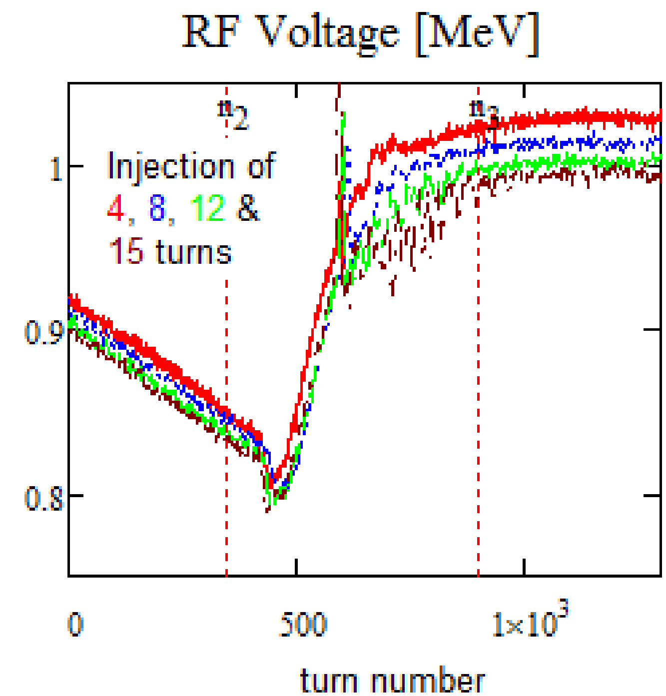

Points presented on the plot are computed by averaging between n_1 and n_2 for data before transition and n_3 and n_4 after transition. An addition due to voltage drop with intensity is subtracted.

Beam Loading

- Accelerating phase shift required by transition crossing changes the beam loading phase and results in a spike in the RF voltage
- Cavity feedbacks mostly suppress the beam induced voltage
  - However short spike of ~150 kV is generated near transition
    - Total shunt impedance of all cavities at transition: R_{sh}=20*145 kΩ
    - Corresponding beam induced voltage (0.5 A) * R_{sh} = 1.5 MV

      ⇒ Suppression is about 10 times

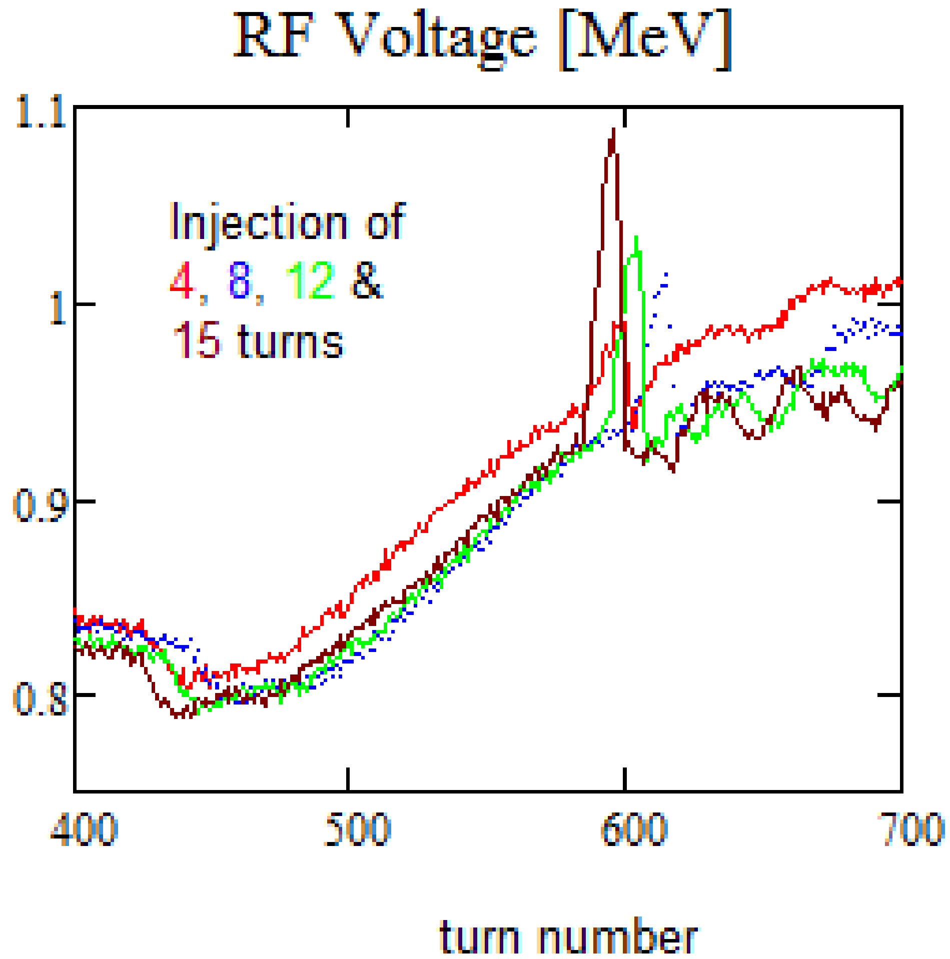

Accelerating Phase Swing Near Transition

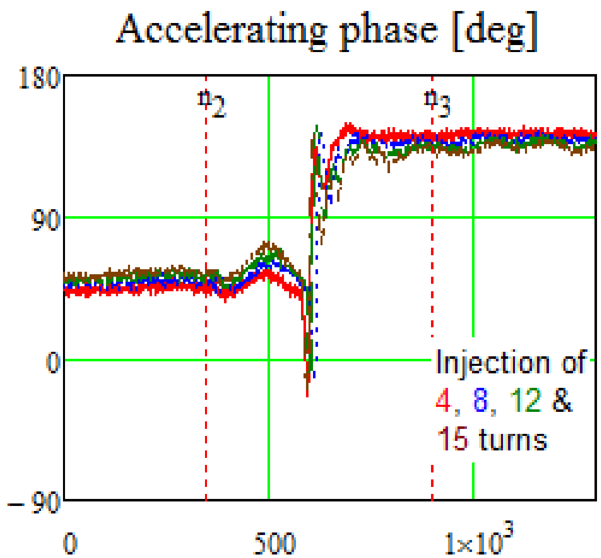

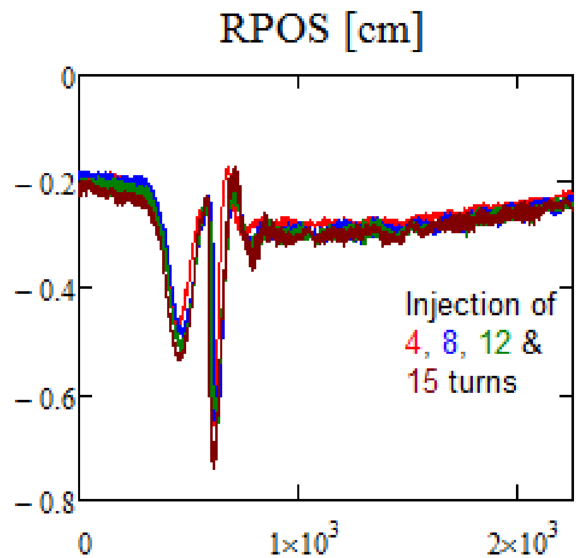

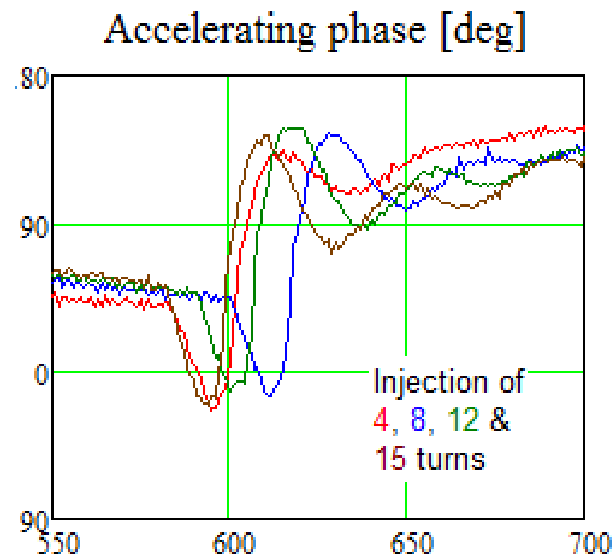

- Accelerating phase experiences very large variations near transition (phase swing)
- For about 10 turns the phase is turned to deceleration
- This phase swings results in considerable droop in beam energy clearly see at RPOS

Bunch Length and Peak Detector

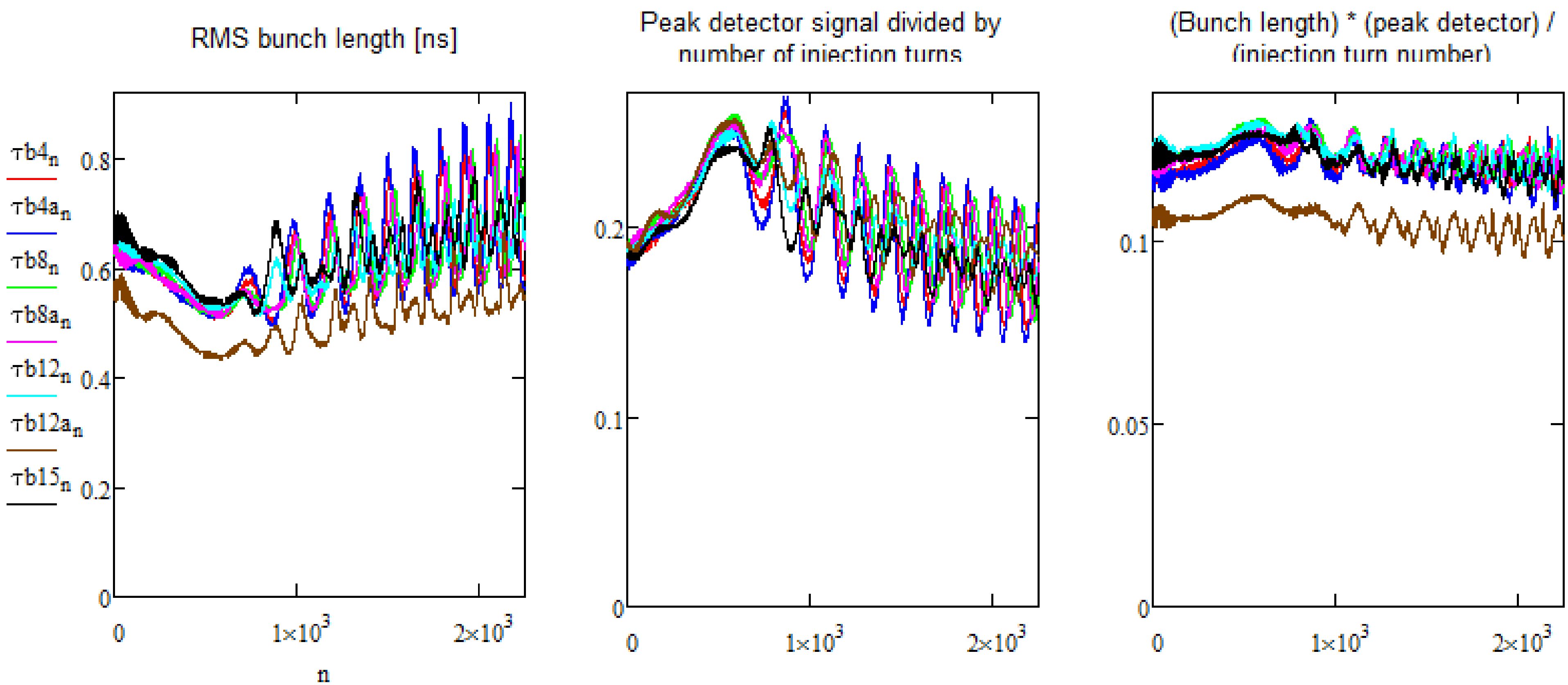

- Bunch length and peak detector are uncorrelated
  - Phase and amplitude of the bunch length oscillations are used to tune simulations to measurements
- Variations of their product are ~5 times smaller but not constant
  - Possible sources are the dispersion in cable and finite time resolution of Resistive Wall Monitor

Bunch and RF Frequencies

- Dependencies of bunch and RF frequencies on time verify timing of the transition crossing measurements
- Variations of RPOS do not produce detectable changes in bunch frequency
- It yields limitations on the slip factor value ($\eta<2\cdot10^{-3}$) and distance from the transition ($\Delta n<250$)
  - Here we use: $\Delta f/f=5\cdot10^{-6}$, $\Delta p/p=2.5\cdot10^{-3}$
- Transition crossing simulations are sensitive to transition crossing location of ~10 turns

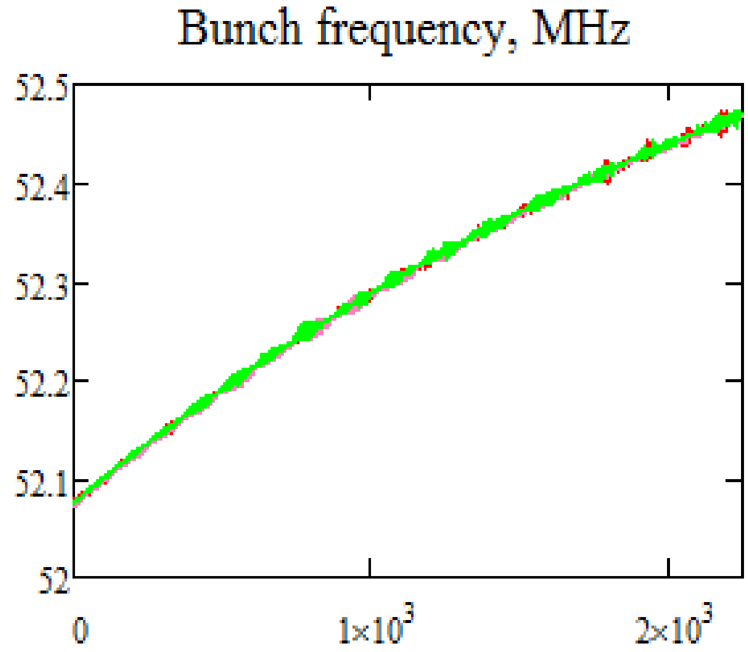

$$\left(\frac{\Delta f}{f}\right)_n = \frac{f_n - \left(f_0 + f_p \cdot n + f_{pp} \cdot n^2\right)}{f_n}$$

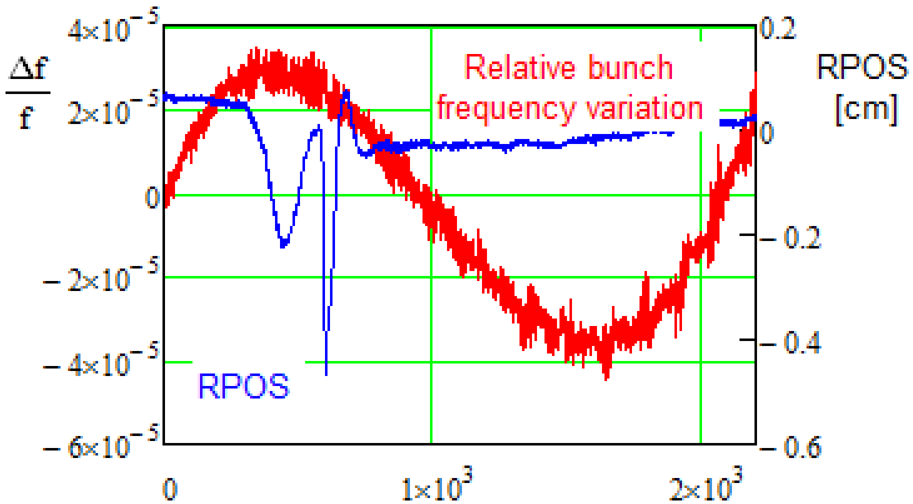

Part 2: Data Analysis and Simulations

Accelerator Physics and Technology Seminar

May 17, 2016

Fermilab

Short Review of Part I

- Resistivity of steel laminations in dipoles makes the major contribution to $Z_L(\omega)$
- Large resistive impedance makes beam deceleration with average rate of ~140 kV/turn for 15 turn injection ($4.8{\cdot}10^{12}$ p)
- Measurements
  - Data from RF sum, Resistive Wall monitor and RPOS were acquired at injection and near transition at different intensities
    - Digital scope (0.8 ns sampling time, 3.5 ms trace duration)
  - Data analysis yielded dependencies on time for: bunch length, bunch peak current, RF voltage, actual accelerating phase, relative momentum deviations
  - Data analysis presented below resulted in calibrations for RPOS, RF sum and accelerating phase

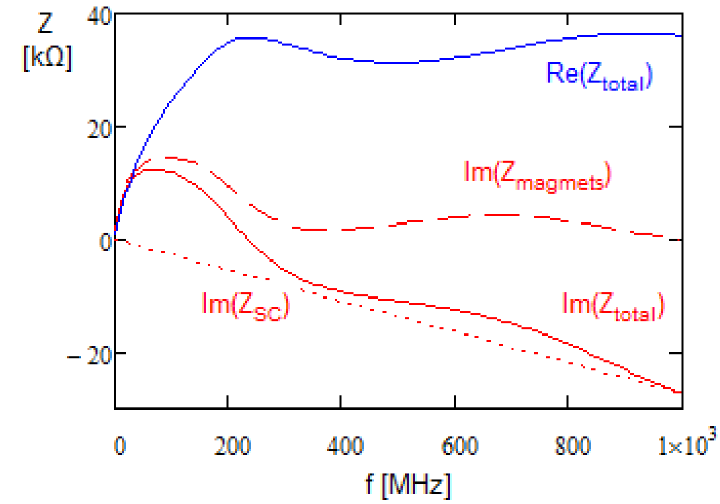

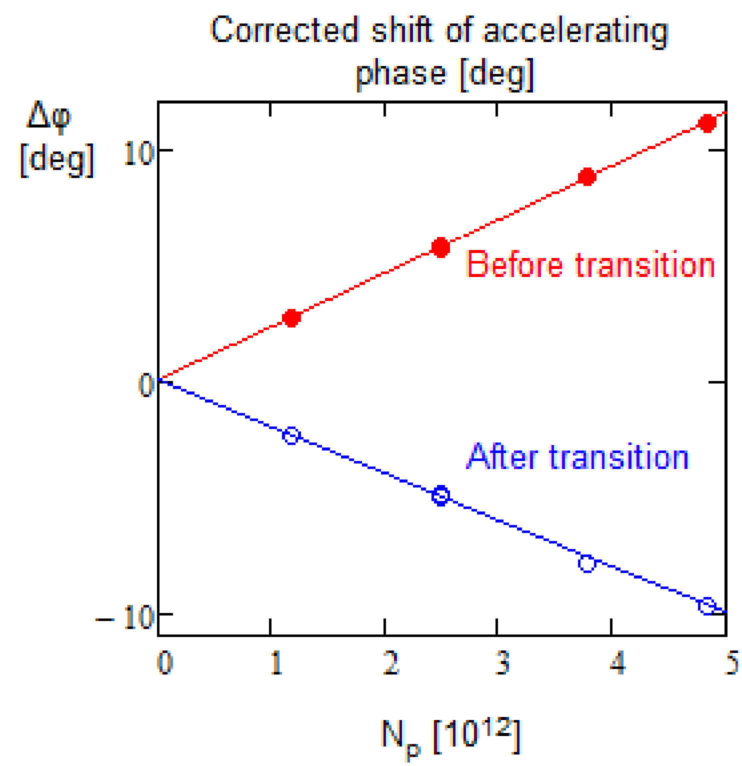

Phenomenological Model for Data Analysis

- Reference beam energy at each turn is determined by magnetic field in dipoles: $B(t) = \frac{B_{max} + B_{min}}{2} + \frac{B_{max} - B_{min}}{2}\cos(\omega_{ramp} t)$
- Beam energy growth is driven by

$$\mathrm{E}_{n+1} = \mathrm{E}_n + e\left(V_0 \sin\left(\varphi_{acc_n}\right) - V_{beam_n}\right), \quad V_{beam_n} = \frac{A_V N_p}{\tau_{b_n}}$$

- The difference yields the momentum deviation which is independently measured by RPOS
- A presence of fast RF phase swings near transition greatly helps us to calibrate (1) RF voltage sum, (2) offset of accelerating phase, (3) RPOS and (4) find average beam decelera-tion due to impedance
  - Differnce is extremly sensitive to minor change in parameter values

$\kappa_{RF} = 1.806$ $\varphi_{ofs} = -51.502$ deg $\tau_d = 1.577 \times 10^{-6}$ s $V_{bt} = 8.1 \times 10^3$

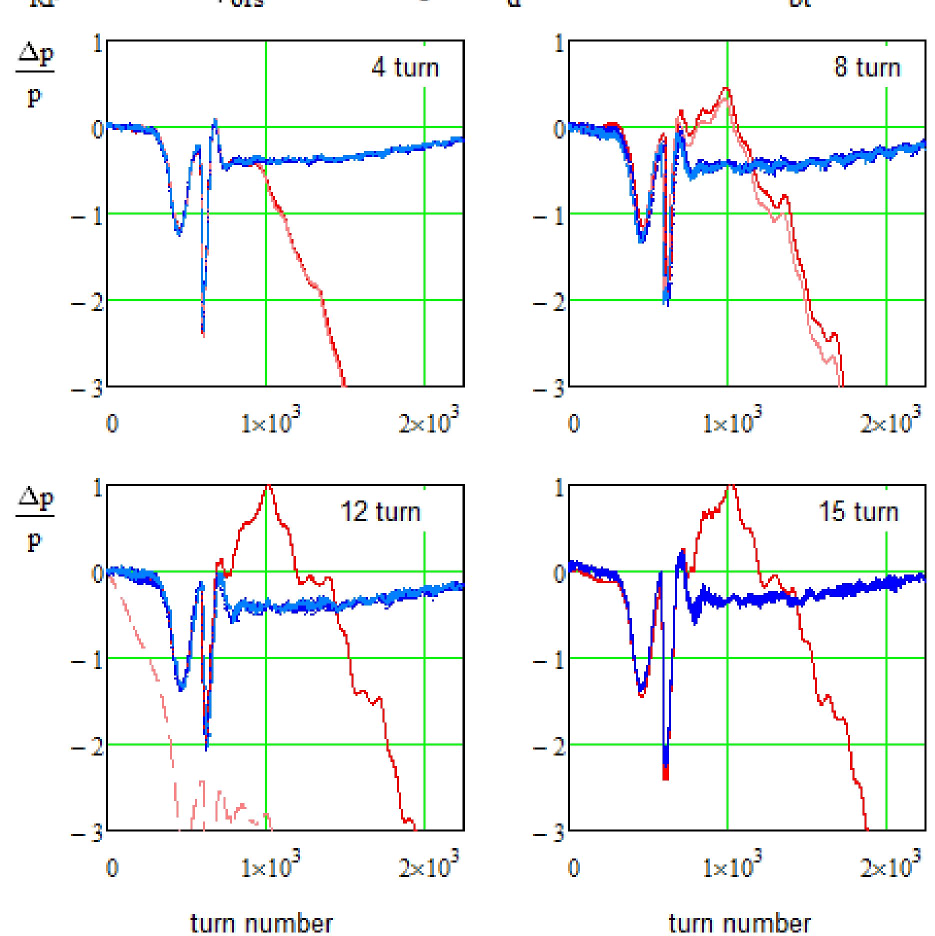

Parameters are fitted for the first 900 turns of 4 turn data

Phenomenological Model for Data Analysis (2)

- Fitting the entire set of data does not make significant changes for calibration of RF voltage and phase
  - RF voltage calibration is well within 1% and RF phase within 1 deg.
  - It is sufficient for transition crossing simulations
- Due to error accumulation such analysis is extremely sensitive to errors
- Actual reason for discrepancy is unknown: asymmetry of potential well, dispersion in cable can make minor changes in accelerating phase correlated with bunch length, …

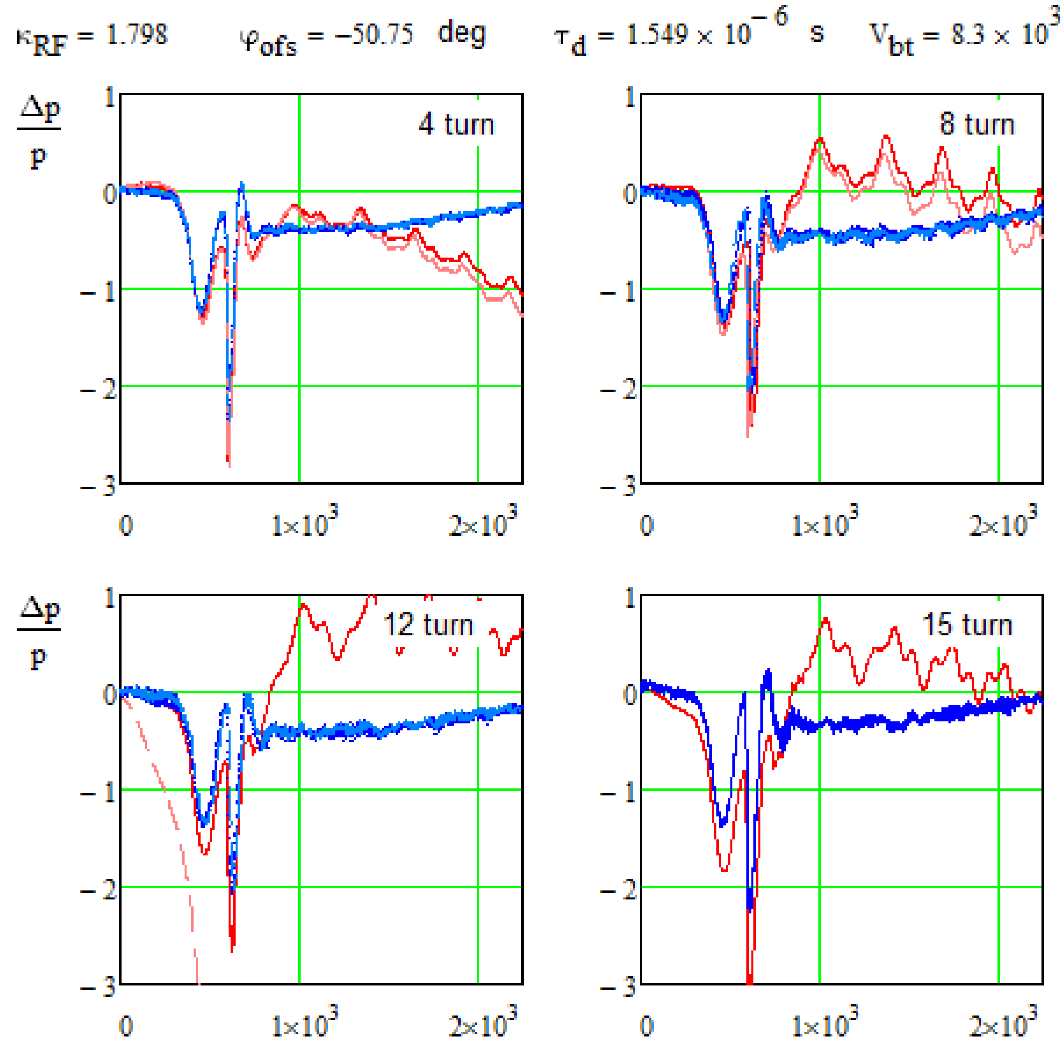

Parameters are fitted for the entire sets of 4 and 15 turn data

Signal Calibrations Resulting from Data Analysis

- Data analysis yields following calibrations near transition:
  - Total RF voltage: $V_{peak}=(1.8\pm0.01)\cdot10^7\ V_{RFsum}$
  - Calibration of RPOS for $\Delta p/p$: $\Delta p/p = 0.067 * RPOS_{(V)}$
    - ~1.25 times smaller than expected (D=180 cm, dx/dV = 15 cm/V) corresponding to D_{eff}=225 cm
  - Peak decelerating voltage average over the beam distribution is ~140 kV for 15 turn injection
- Voltage calibration at injection cannot be accurately derived from the data
  - It is determined by quality of RF sum circuit and is unknown
  - The same voltage calibration as at transition is assumed
- RPOS calibration at injection is different due to optics changes but it is insignificant for numerical simulations

Decelerating voltage induced by impedance, kV

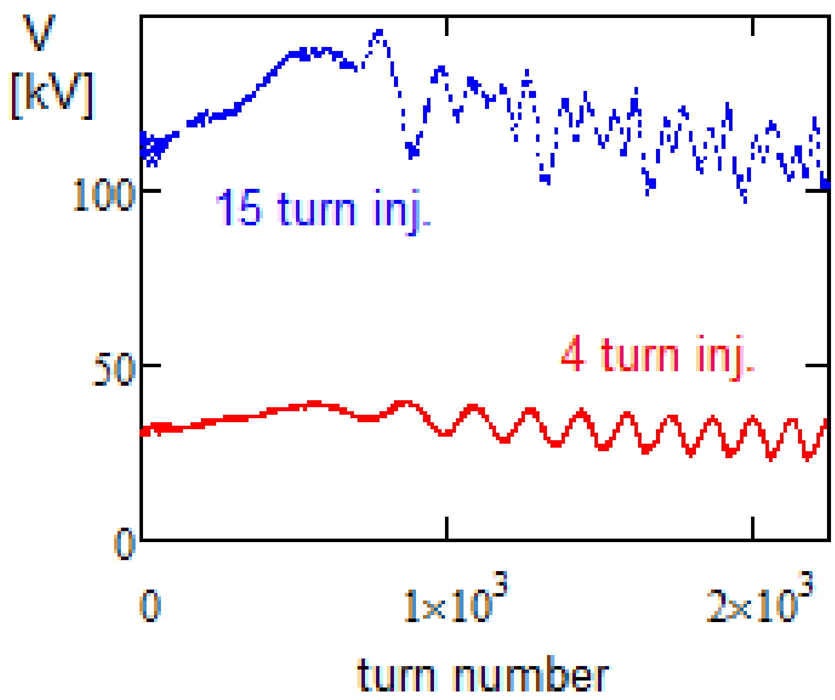

Measurements of Adiabatic Bunching

- Bunching takes about 50 turns yields the longitudinal emittance
- Dependence of bunch frequency on time yields time of magnetic field minimum and injection energy for the reference particle (as well as the energy of injected beam)
  - Typically Bmin is achieved at turn ~40
- After bunching the bunch profile is close to a Gaussian with slightly truncated tails
  - Fall time is increased due to dispersion in the cable and finite resolution time for RWM, and asymmetry of RF bucket due to acceleration (opposite effect after X)
  - Lumpiness resulting from injection are well observed to about turn 600

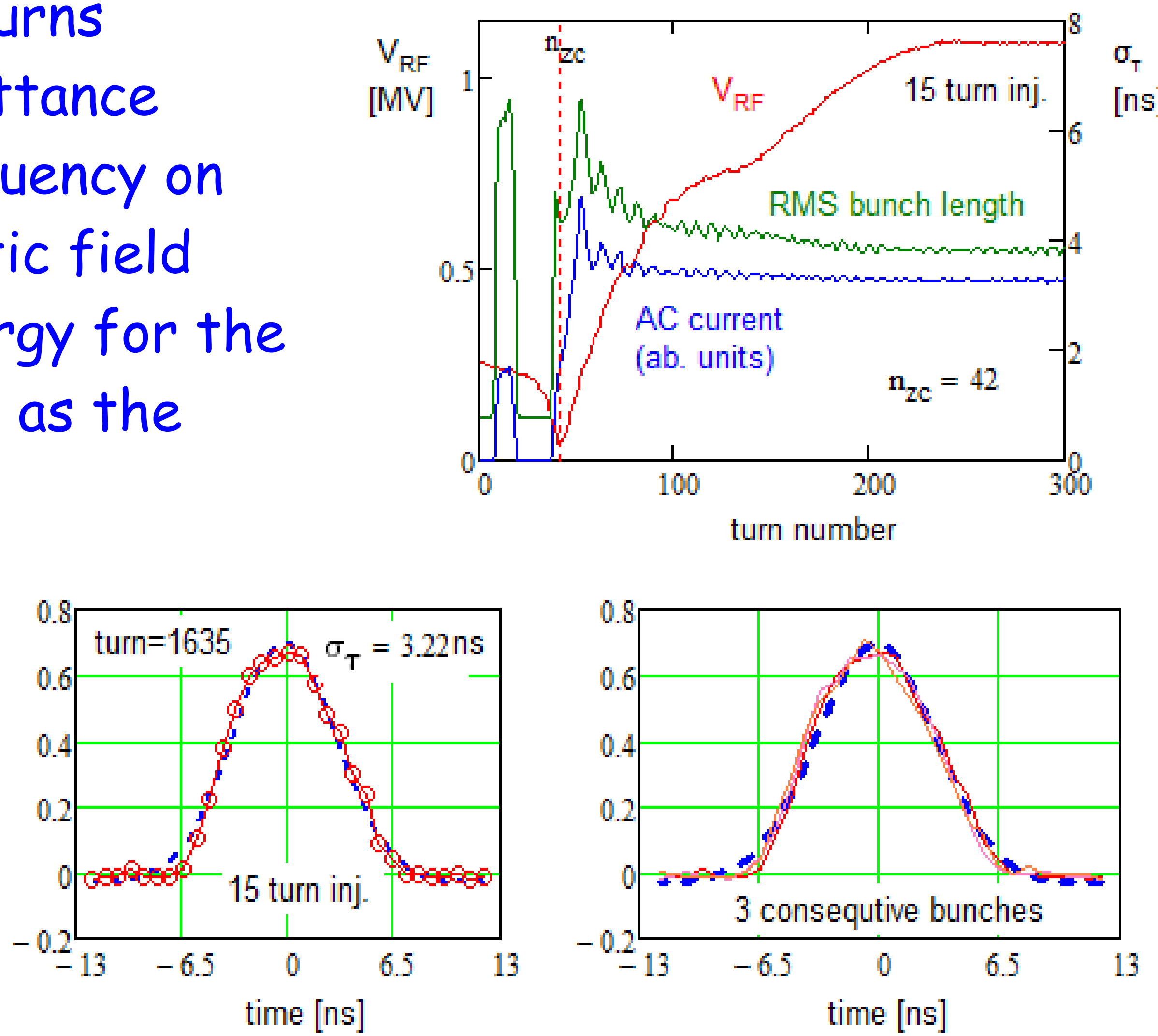

RF Voltage for Numerical Simulations

- RF wave form is built from measured RF voltage at inj. & around X
- RF wave form was interpolated for the rest of the cycle
  - ♦ Minor inaccuracies of interpolation are irrelevant to simulations
  - ♦ There is about 10% discrepancy between RF sum measured directly with scope and delivered by Control system
    - Origin has to be traced down
- Time of transition wave form was adjusted relative the transition crossing time based on simulation results

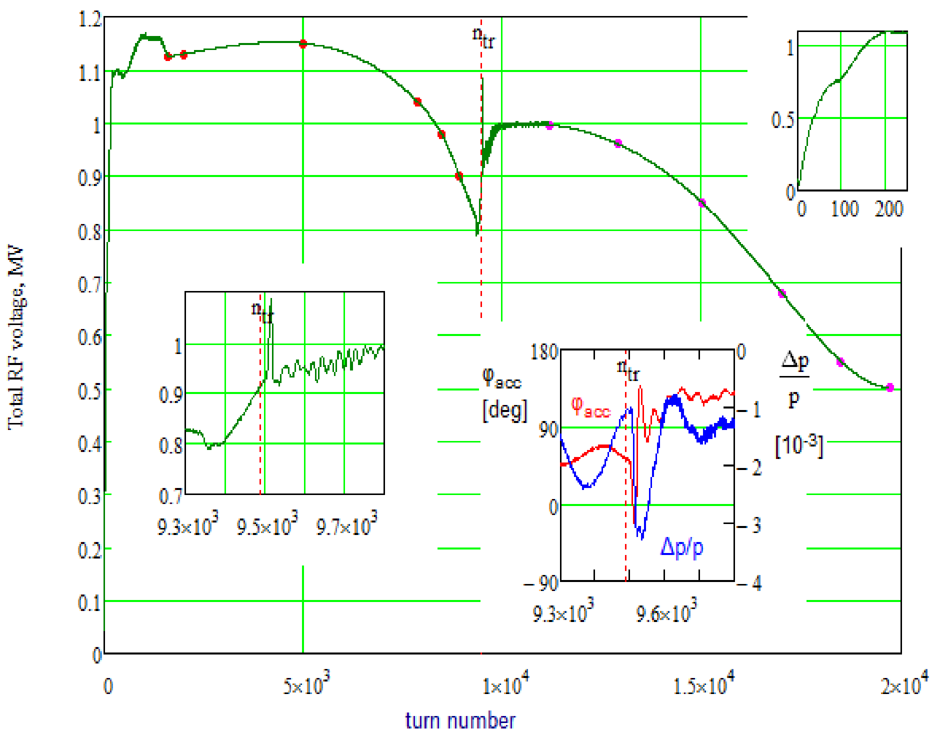

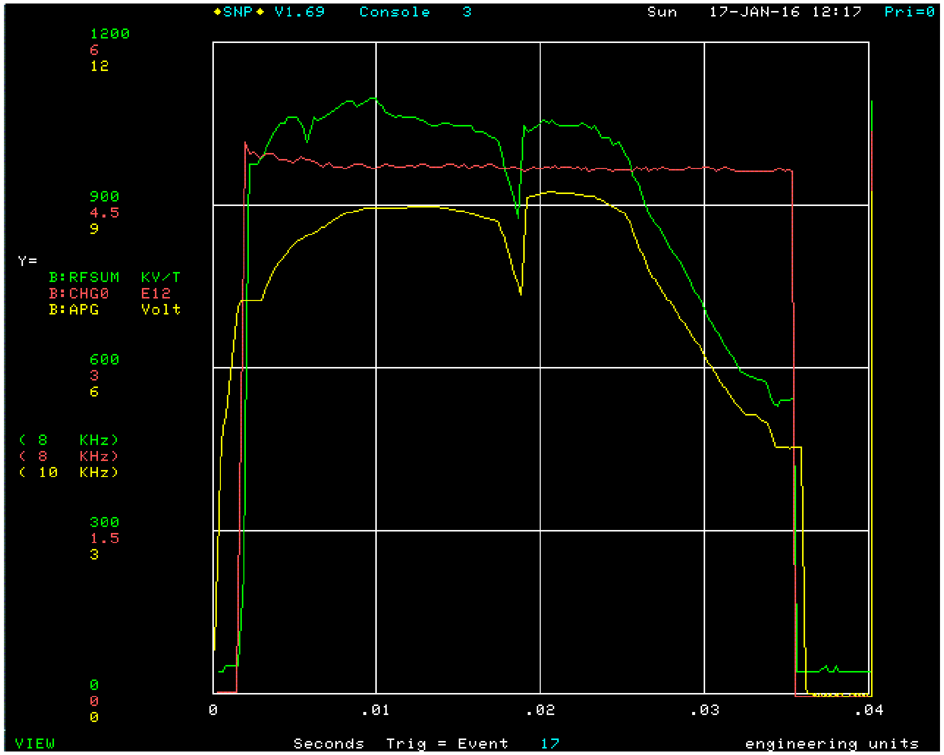

RF Frequency in Numerical Simulations

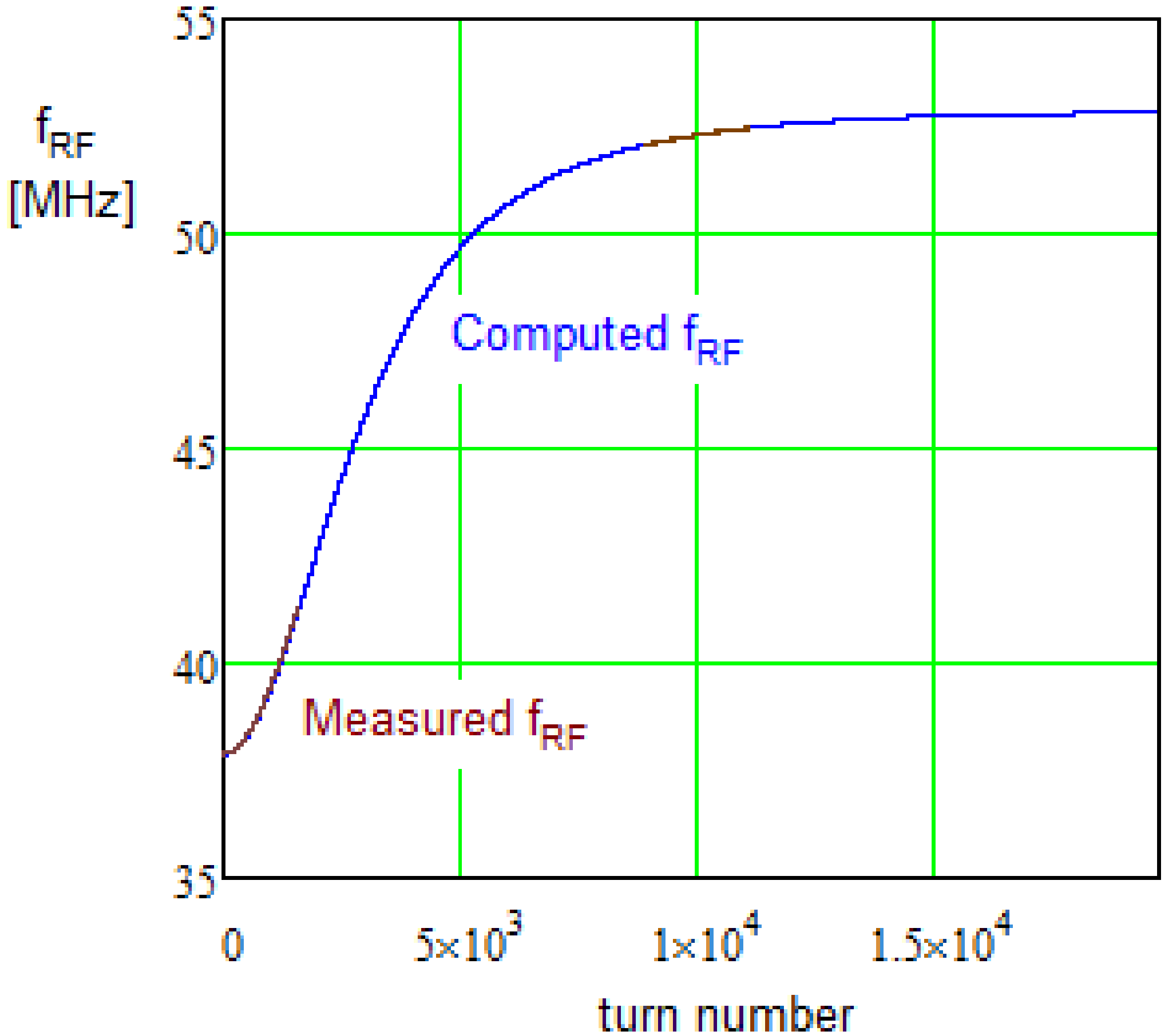

- Measured RF frequency well coincides with the model for injection and extraction energies of 0.400 and 8 GeV

Simulation Program

- Combination of C-program (computations) and MathCad (GUI)
- Accounts for impedances of dipoles and space charge
  - Implies 84 equal intensity bunches
  - Impedances of dipoles is calibrated by the measured RF phase with intensity
  - Measurements do not exhibit significant difference in behavior for bunches in vicinity of the abort gap
    - Both impedances (space charge & Res. Wall) are short range
  - Two dampers
    - Dipole – operates similar to RPOS feedback
    - Quadrupole – feedback on oscillations of bunch length
  - Beam can be unstable above transition if dampers are not engaged
    - At large intensity can result in large beam loss (>50%)
- New GUI driven software is at the initial stage (F. Ostiguy)
  - Takes into account accumulated experience
- Simulations for the largest measured intensity (15 turn) are only presented below
- Projections to PIP-II intensity are also discussed

Accelerating Phase in Numerical Simulations

- Beam automatically adjusts correct accelerating phase due to motion adiabaticity
- However it does not work near transition
  - Measured RF phase was used
    - Additionally a numerical dipole feedback kept the beam momentum offset at the measured values (RPOS)

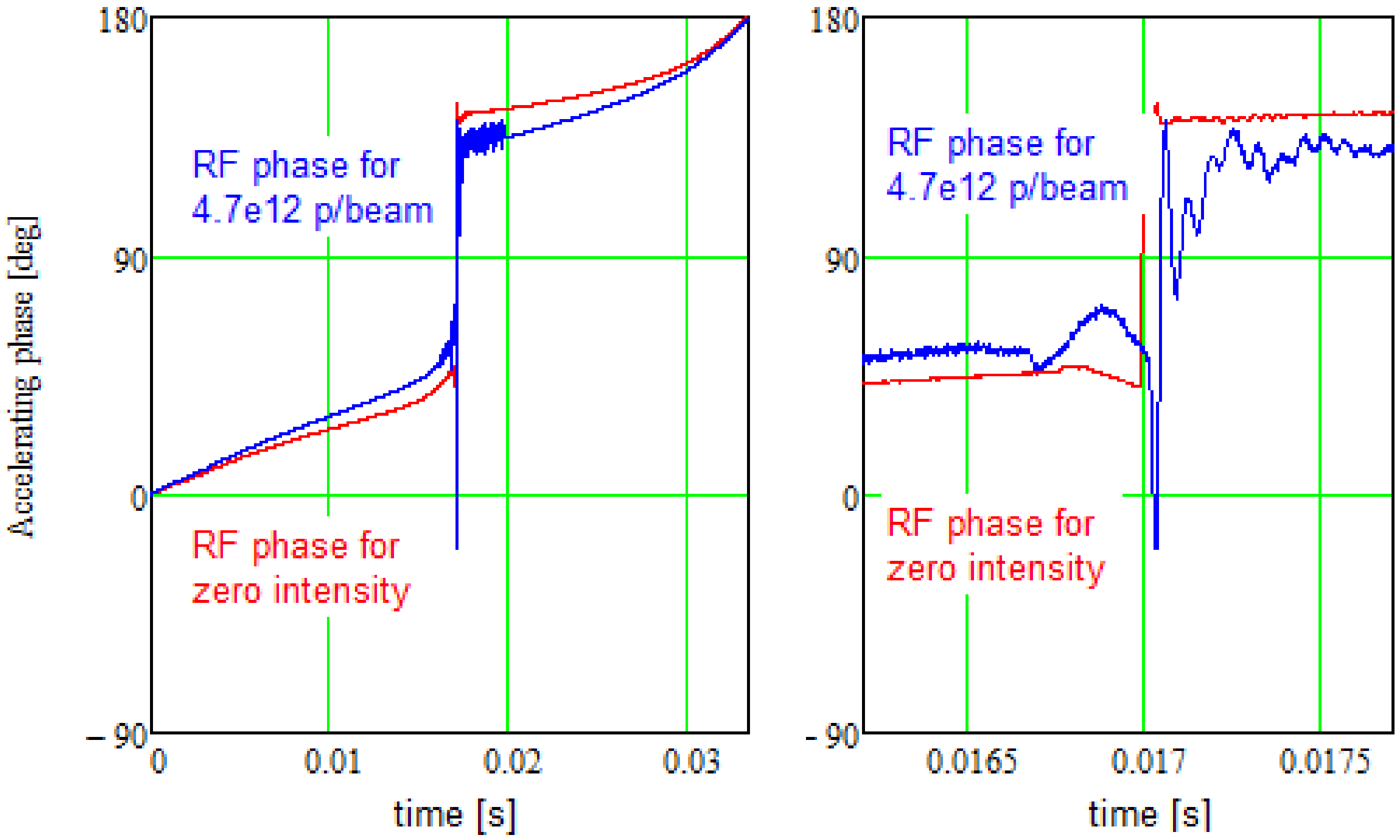

Adiabatic Bunching and Initial Longitudinal Emittance

- Initial long. distribution is Gaussian in momentum with tails truncated at 2.4σ
  - Its width was adjusted to match bunch length measured at injection
  - Beam loss in simulations of 1% is also comparable to what is expected from measurements

Initial momentum distribution used in simulations

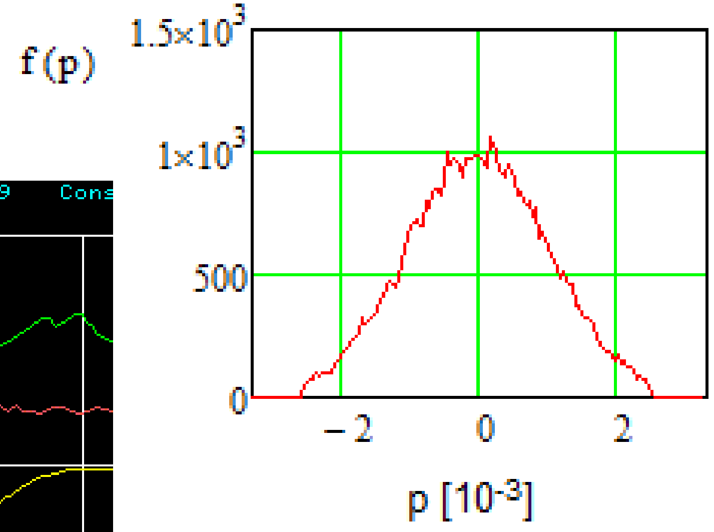

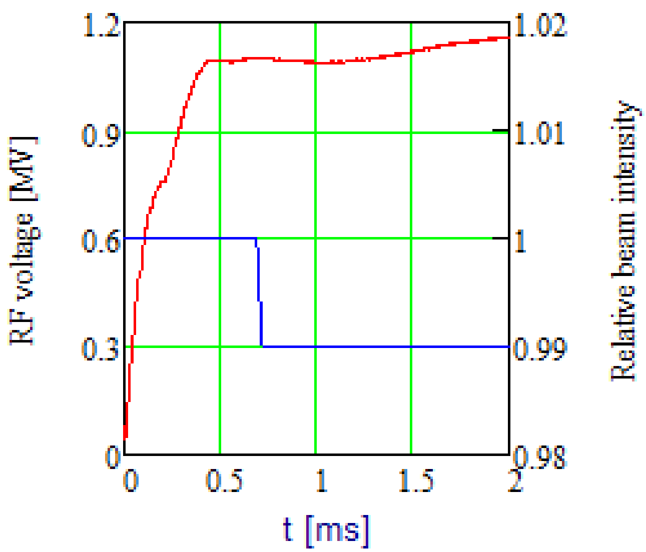

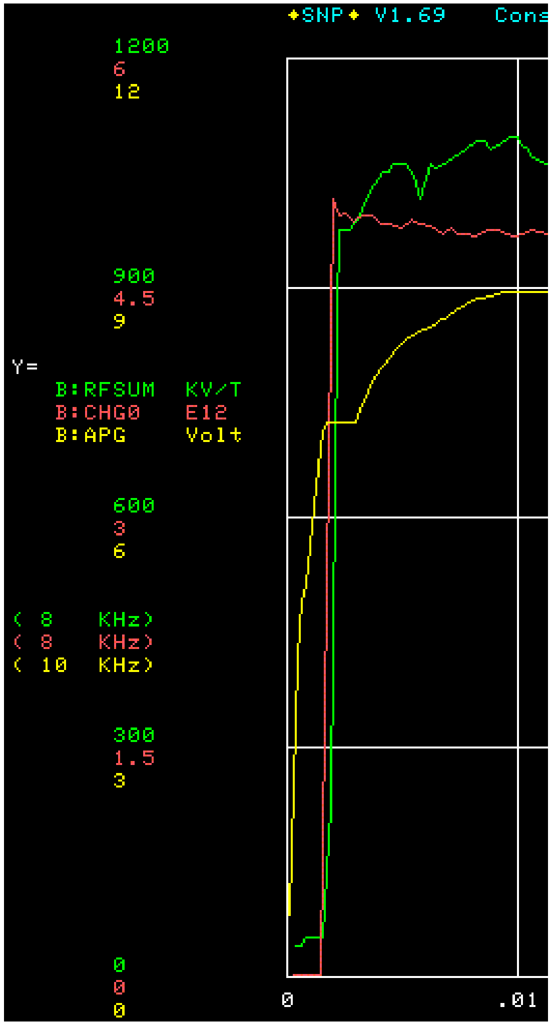

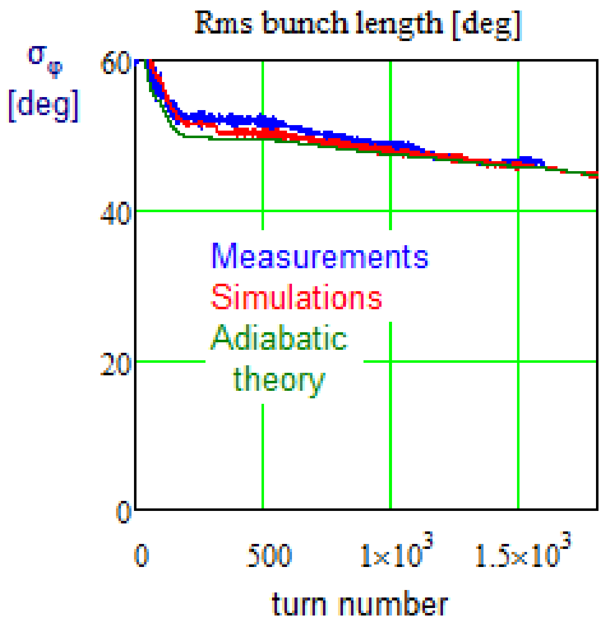

Simulation Results

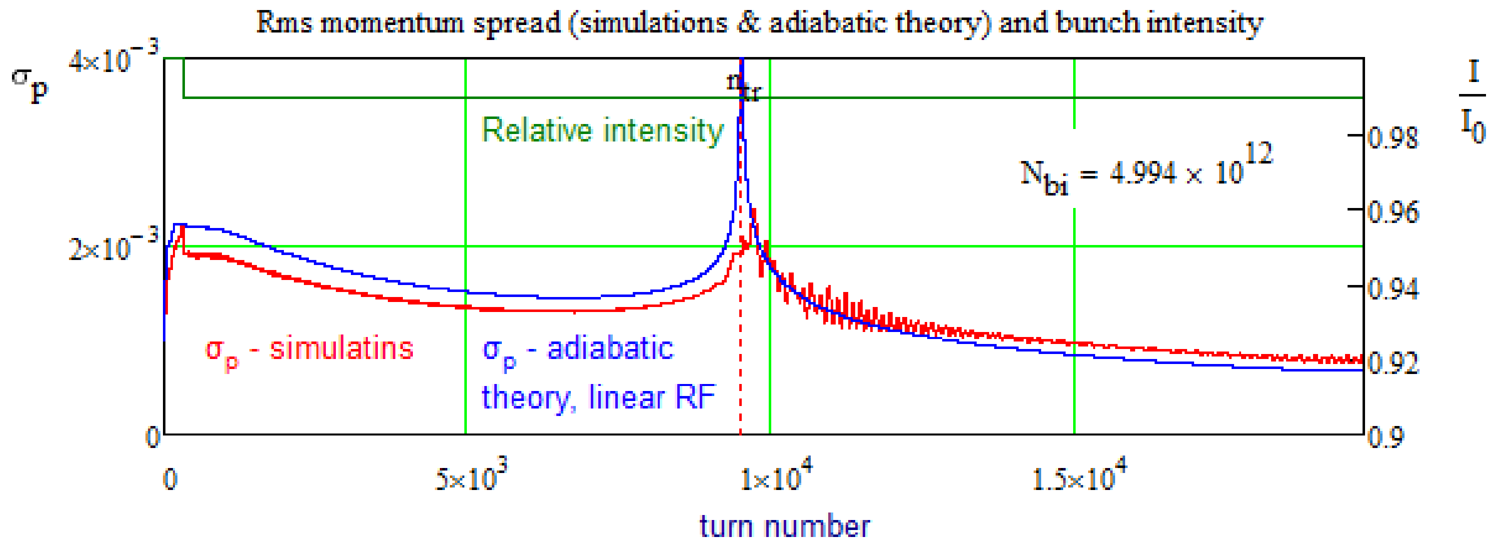

- Same is in the measurements there is no beam loss due to transition

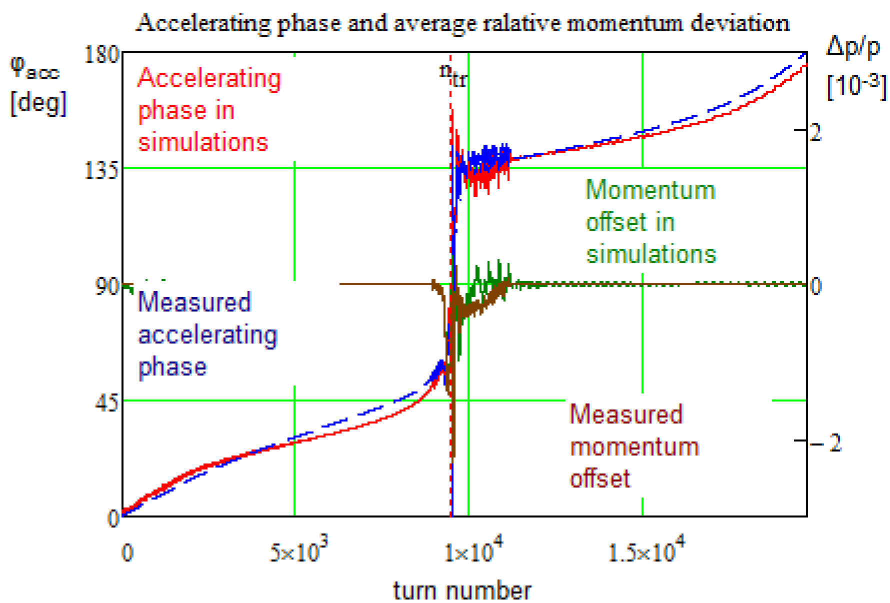

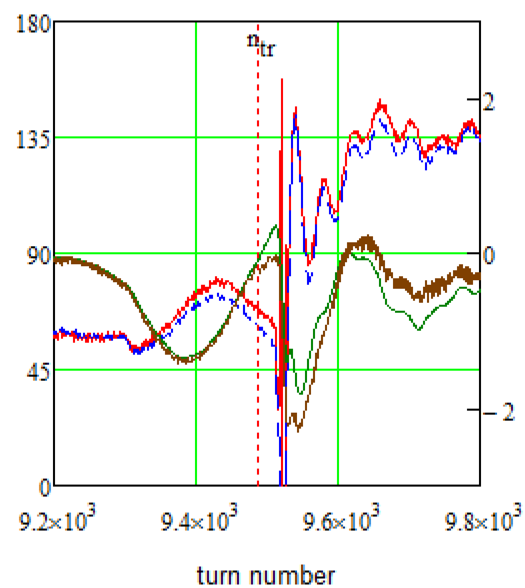

- Momentum offset & φ_{acc} are close in measurements and simulations

Simulation Results (2)

- The accelerating phase shift due to impedance is the same as measured
- The same as in measurements strong suppression of quadrupole oscillations is observed
  - Some discrepancies are still there
  - Non-zero second order slip factor is required to match phase of oscil.

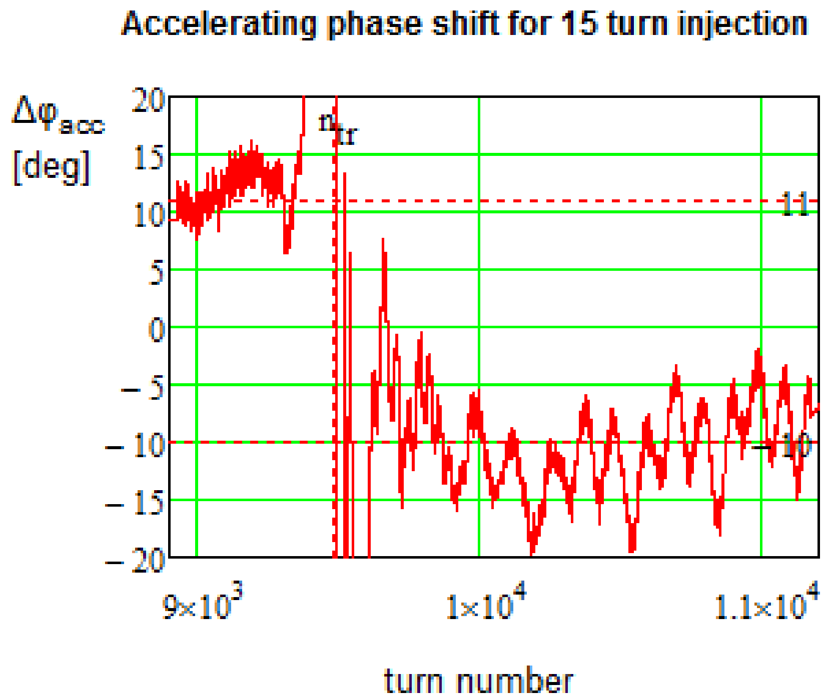

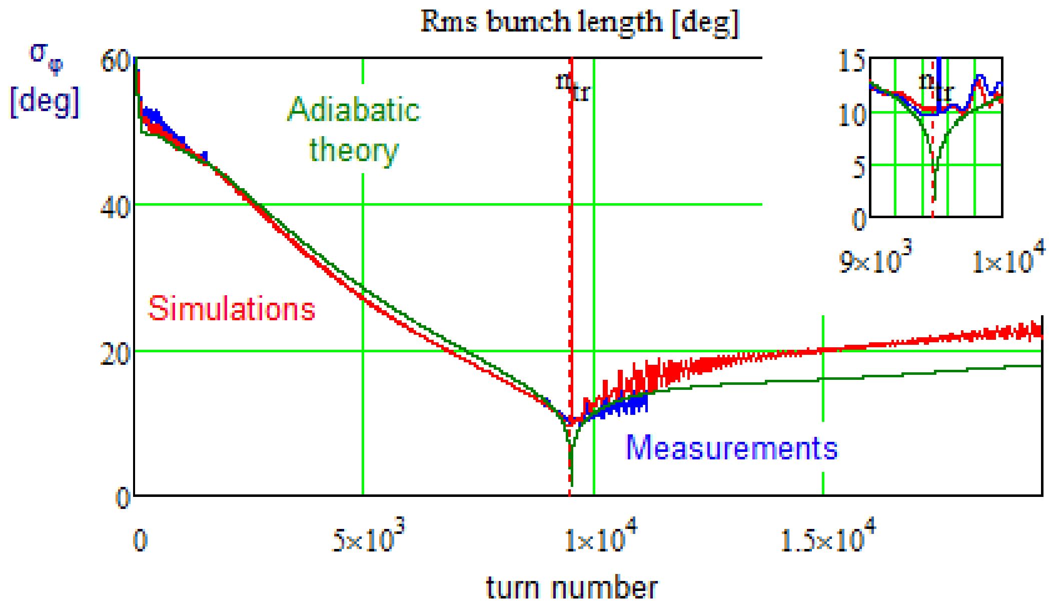

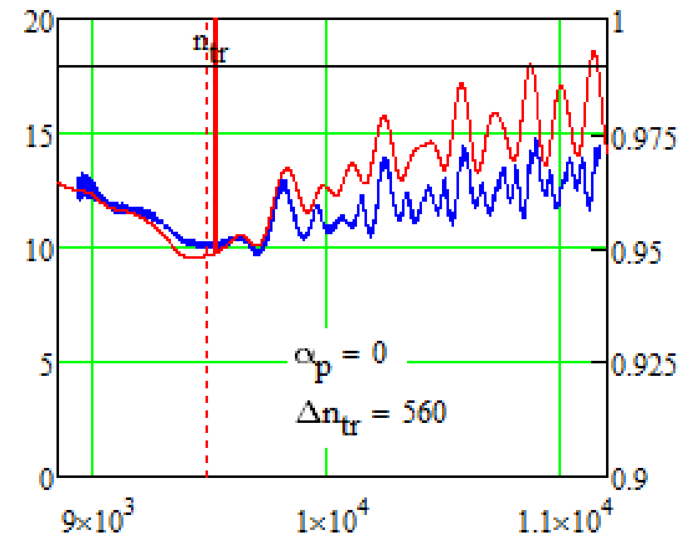

Simulation Results (3)

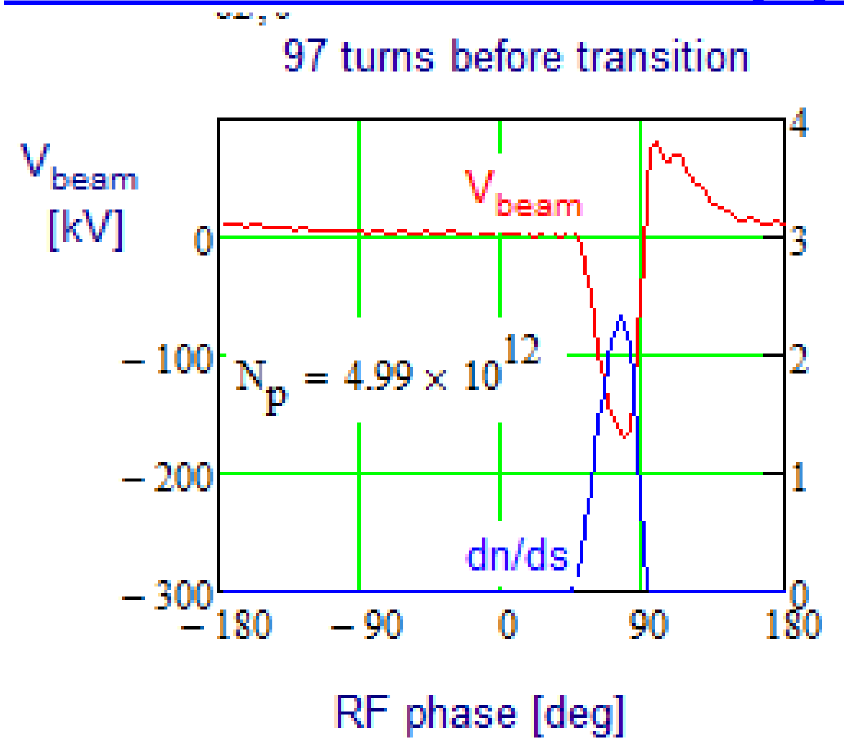

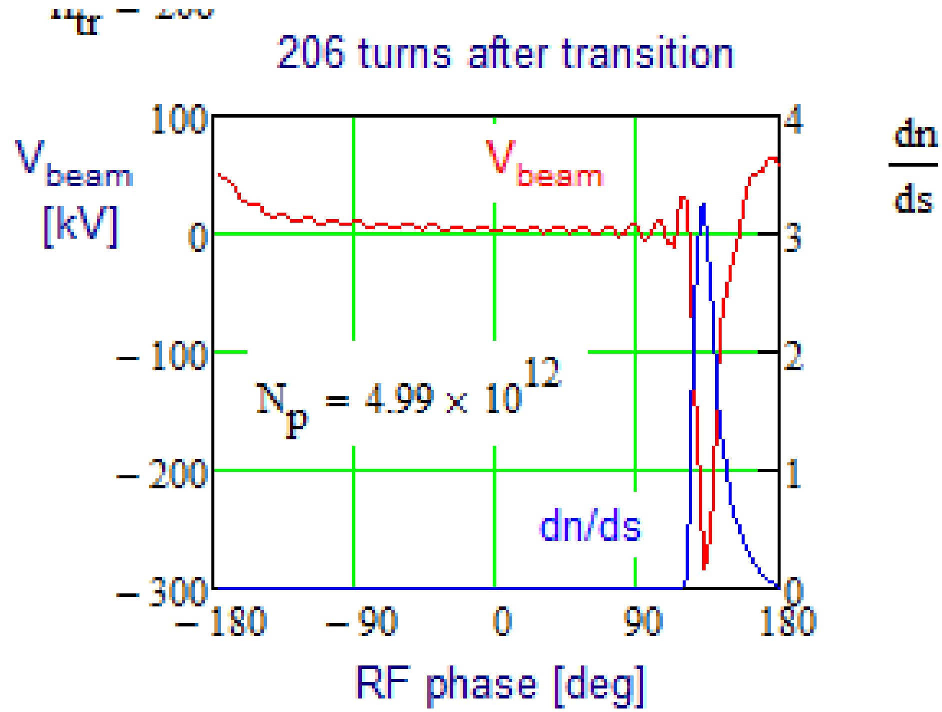

- Shortly after transition
  - Peak decelerating voltage achieves 250 kV/turn
  - Bunch spectrum extends to ~1 GHz

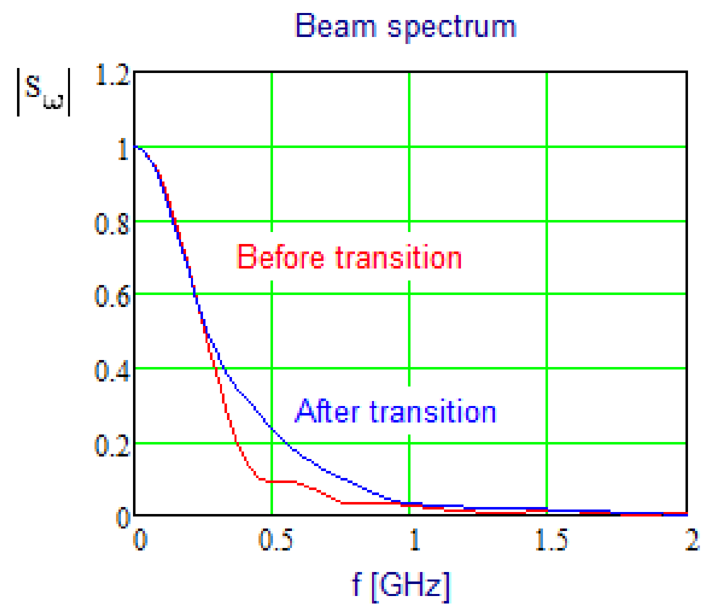

Simulation Results (4)

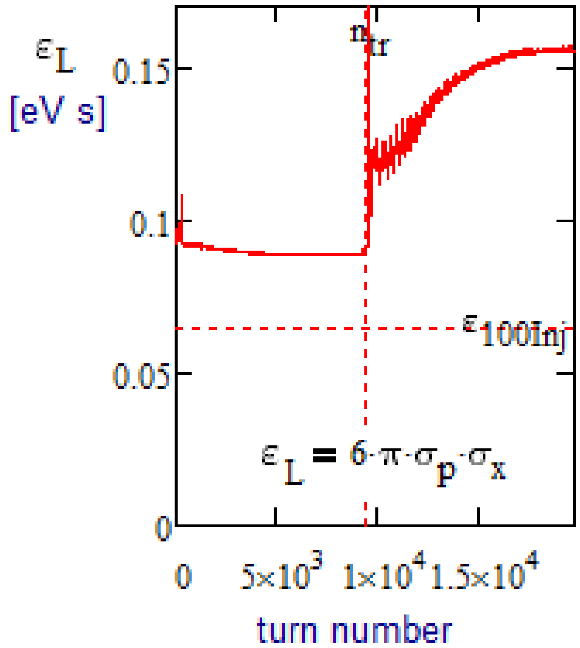

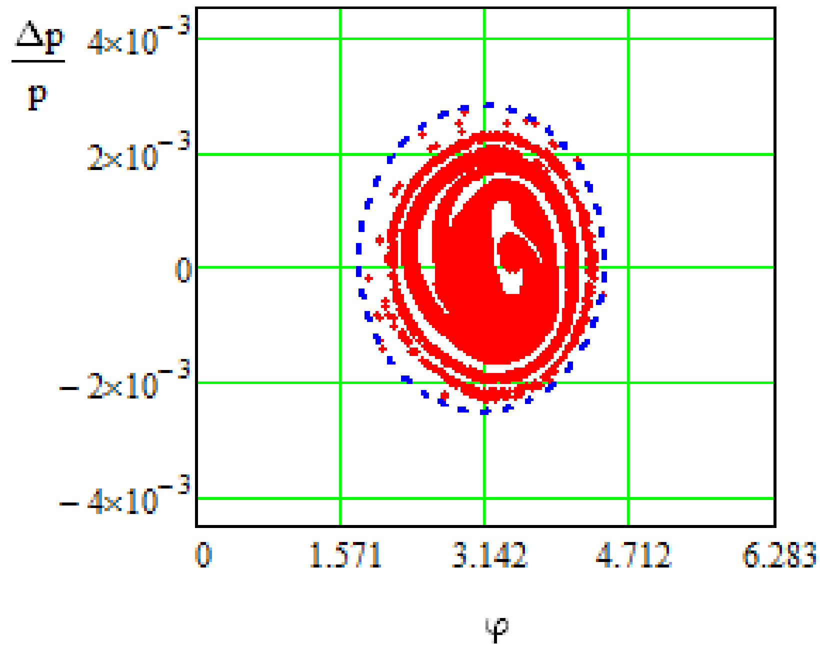

Initial

$\varepsilon_{100Inj} = 0.065$ eV s

Final

$\varepsilon_{100} = 0.295$ eV s

$\varepsilon_{rms} = 0.026$ eV s

$6\cdot\varepsilon_{rms} = 0.157$ eV s

$\frac{\varepsilon_{100}}{\varepsilon_{100Inj}} = 4.542$

- Simulations exhibited moderate emittance growth similar to what we observe in the measurements
  - However simulated RMS bunch length is larger
    - Different accounting for tails?
- Tails are smaller than for the Gaussian distribution with the same RMS emittance

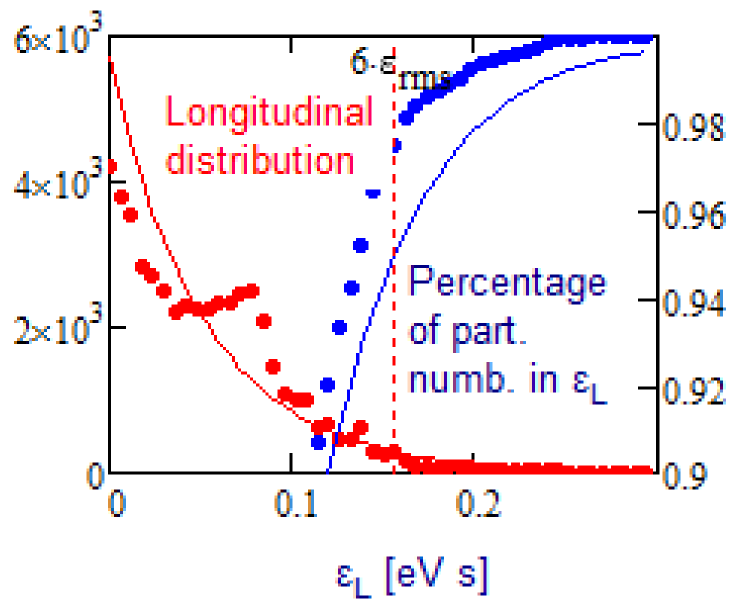

Simulations for PIP-II Intensity: RF Waveform

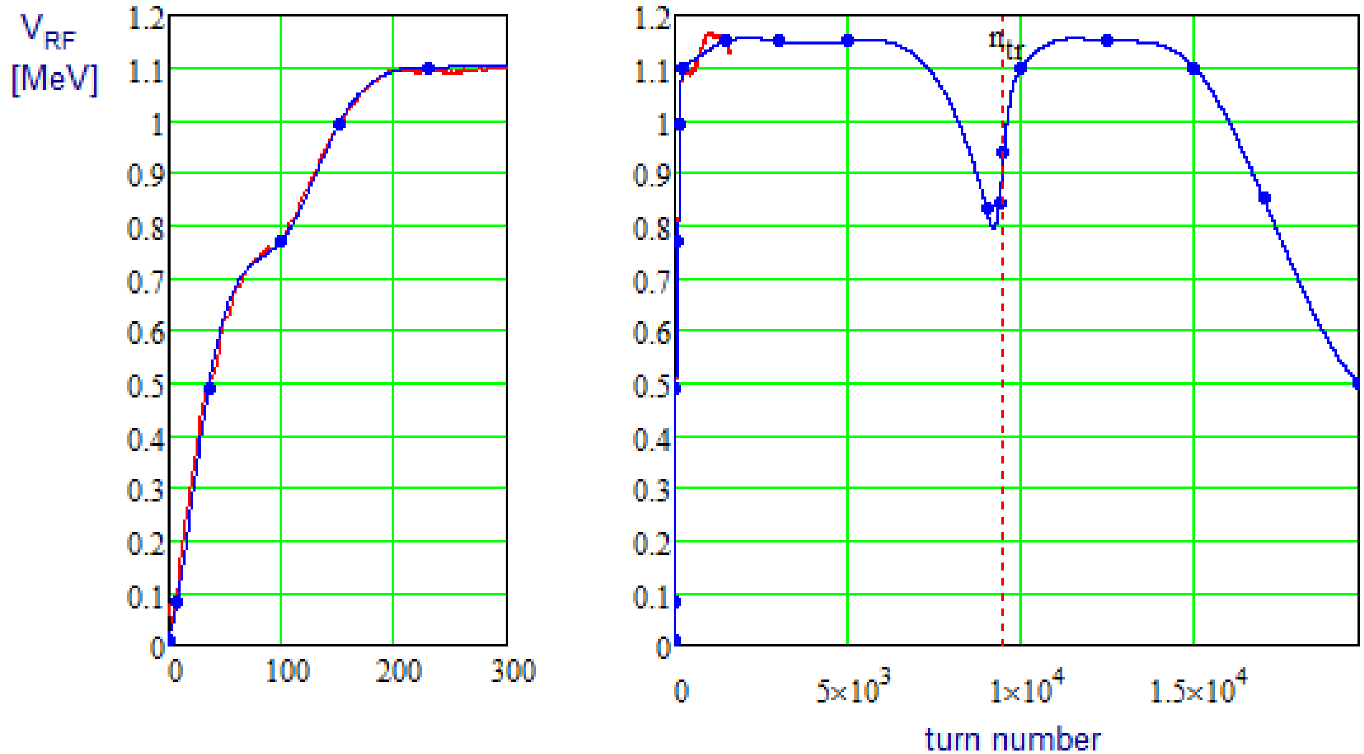

- RF curve is similar to what we have for present Booster
  - Still 15 Hz ramp rate, 1.15 MV maximum
  - No RPOS manipulations,
  - Transition phase jump is delayed by 30 turns
    - Effective remedy to suppress quadrupole oscillations

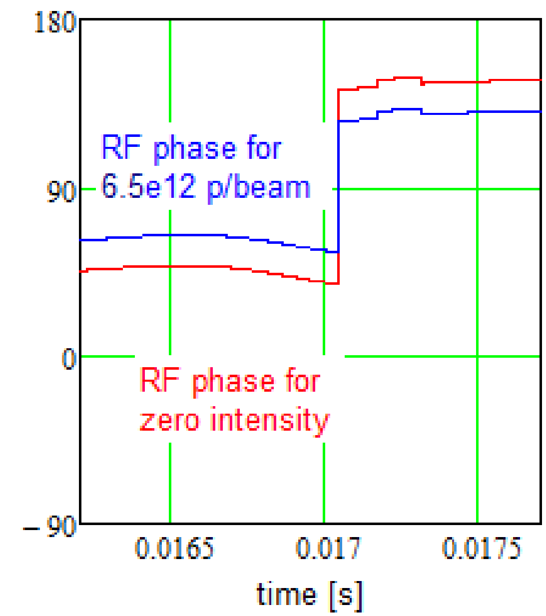

Results of Simulations for PIP-II Intensity

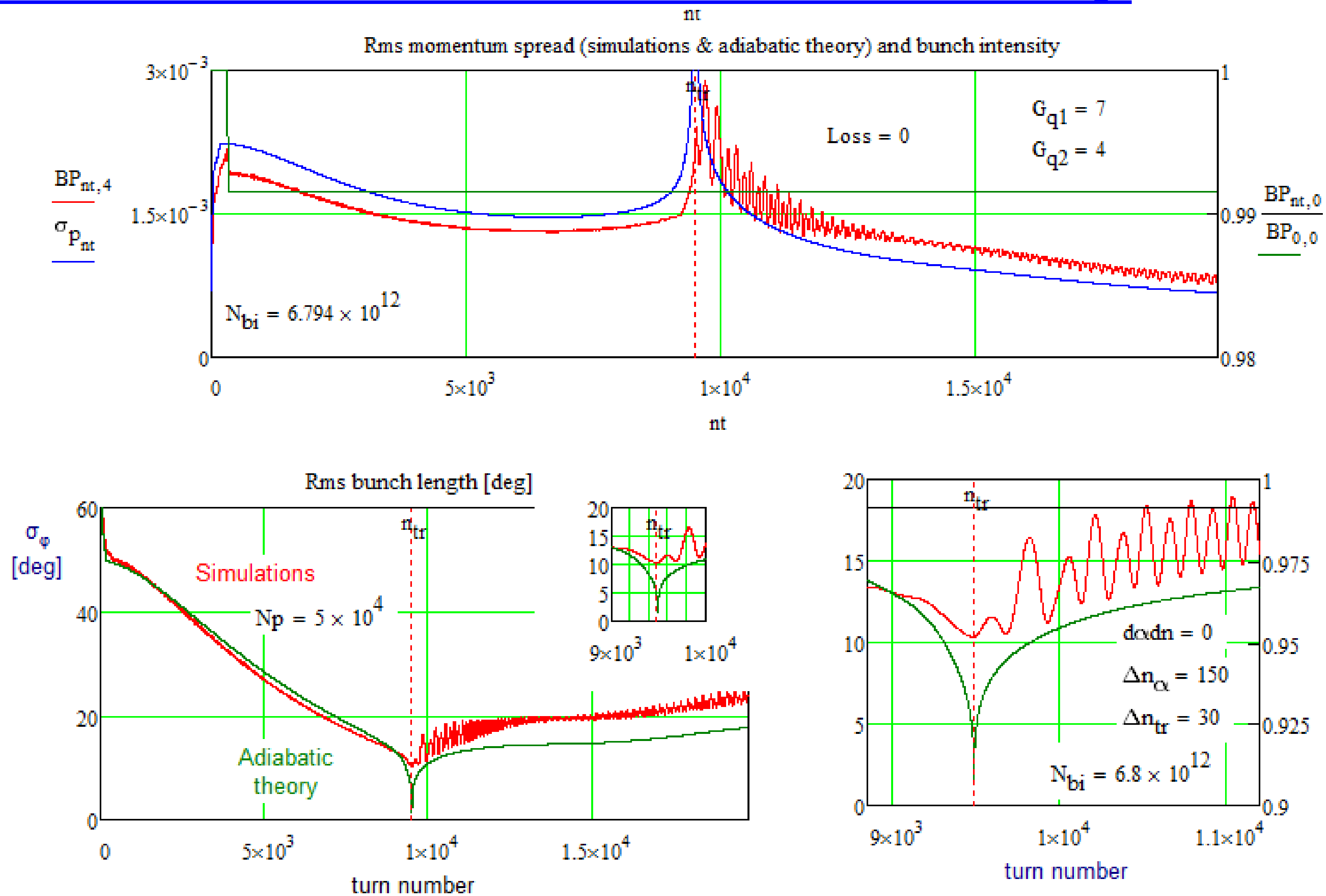

- No beam loss at transition and moderate quadrupole oscillations
- Suppression of quad-oscillations by changing time of RF phase jump does not reduce final emittance but introduce minor beam loss

Results of Simulations for PIP-II Intensity (2)

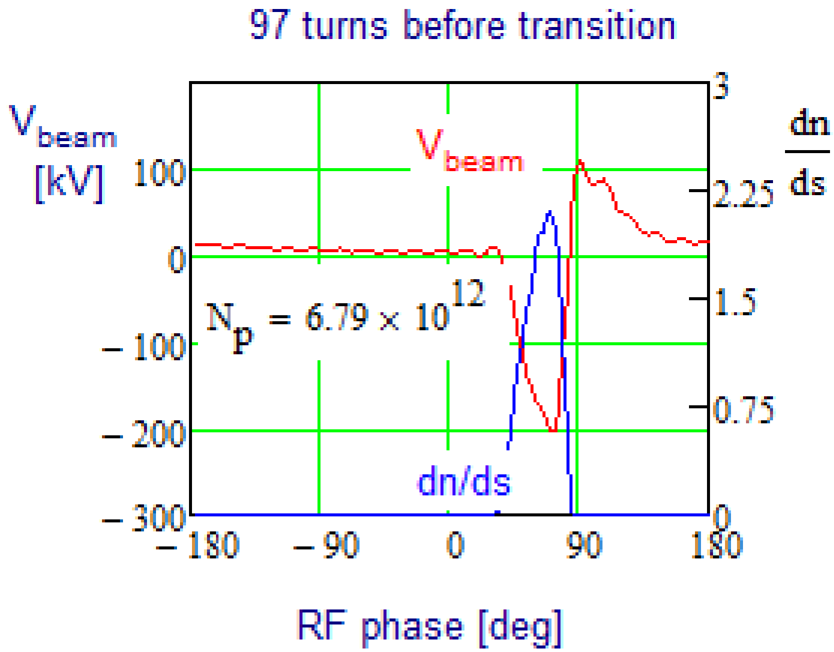

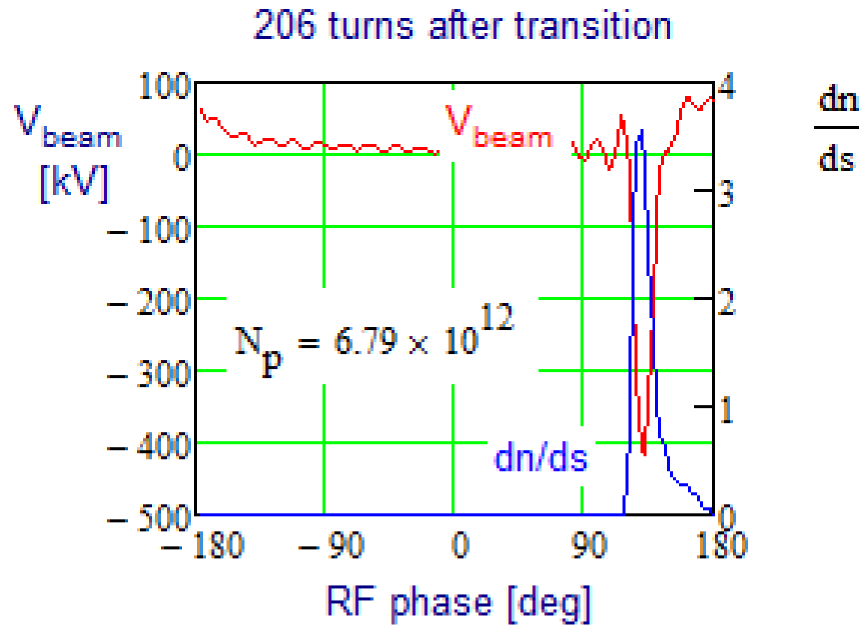

- Peak deceleration voltage grew from ~280 to ~400 kV

Results of Simulations for PIP-II Intensity (3)

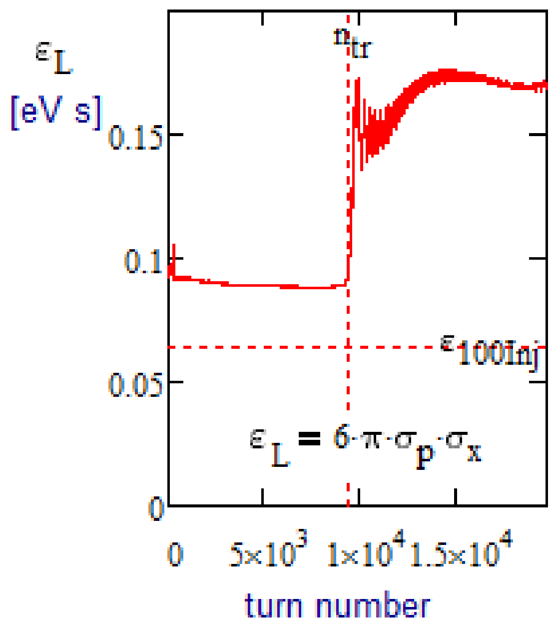

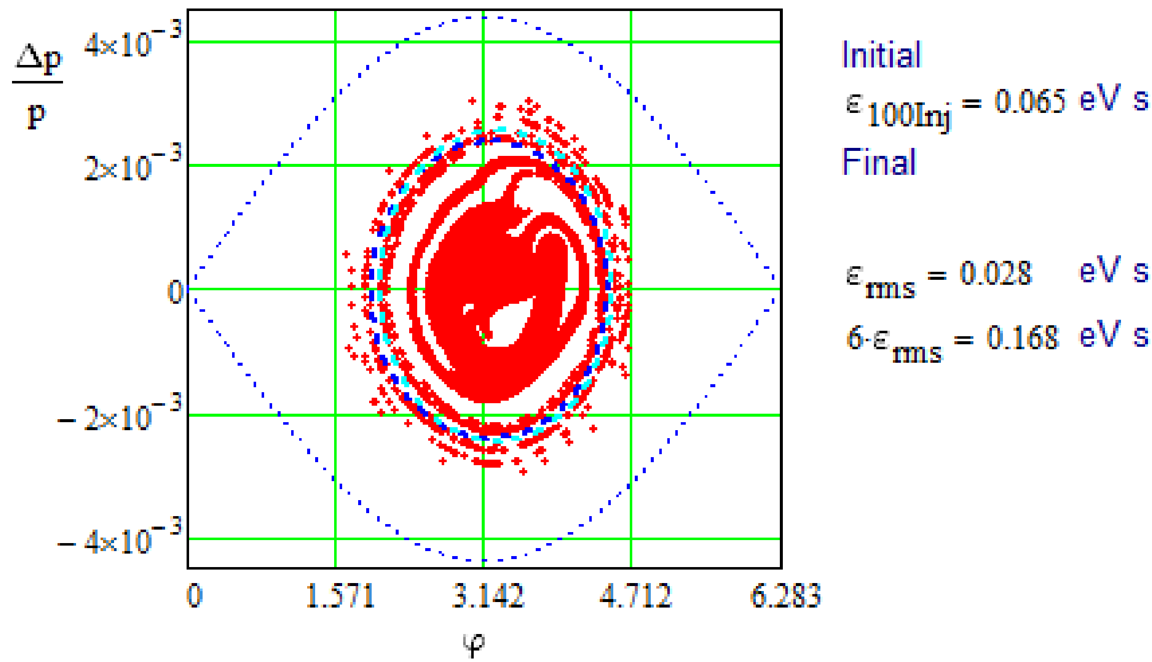

- For PIP-II intensity the rms emittance jump at transition grows in about 2 times
  from (0.09->0.12 eV s, $4.8 \cdot 10^{12}$)
  to (0.09 -> 0.015 eV s, $6.5 \cdot 10^{12}$)
  - Non-Gaussian truncated tails-> Gaussian tails

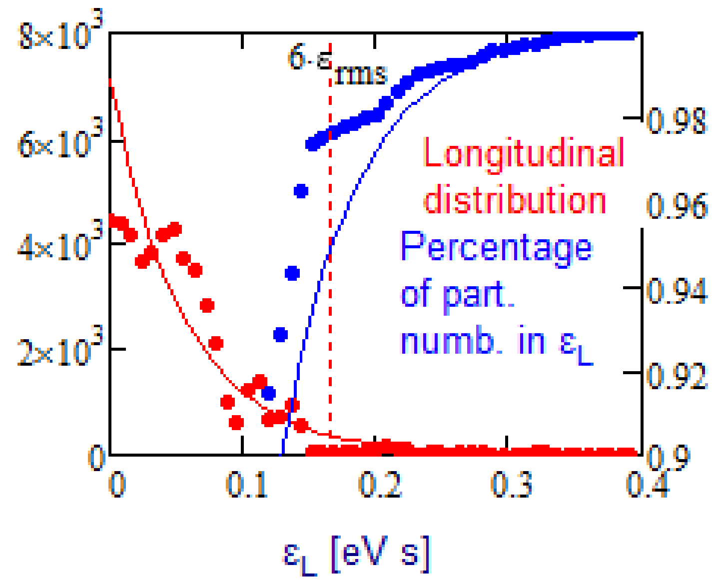

Suppression of Emittance Growth after Transition

- Increase of V_{RF} after transition suppresses the emittance growth after transition

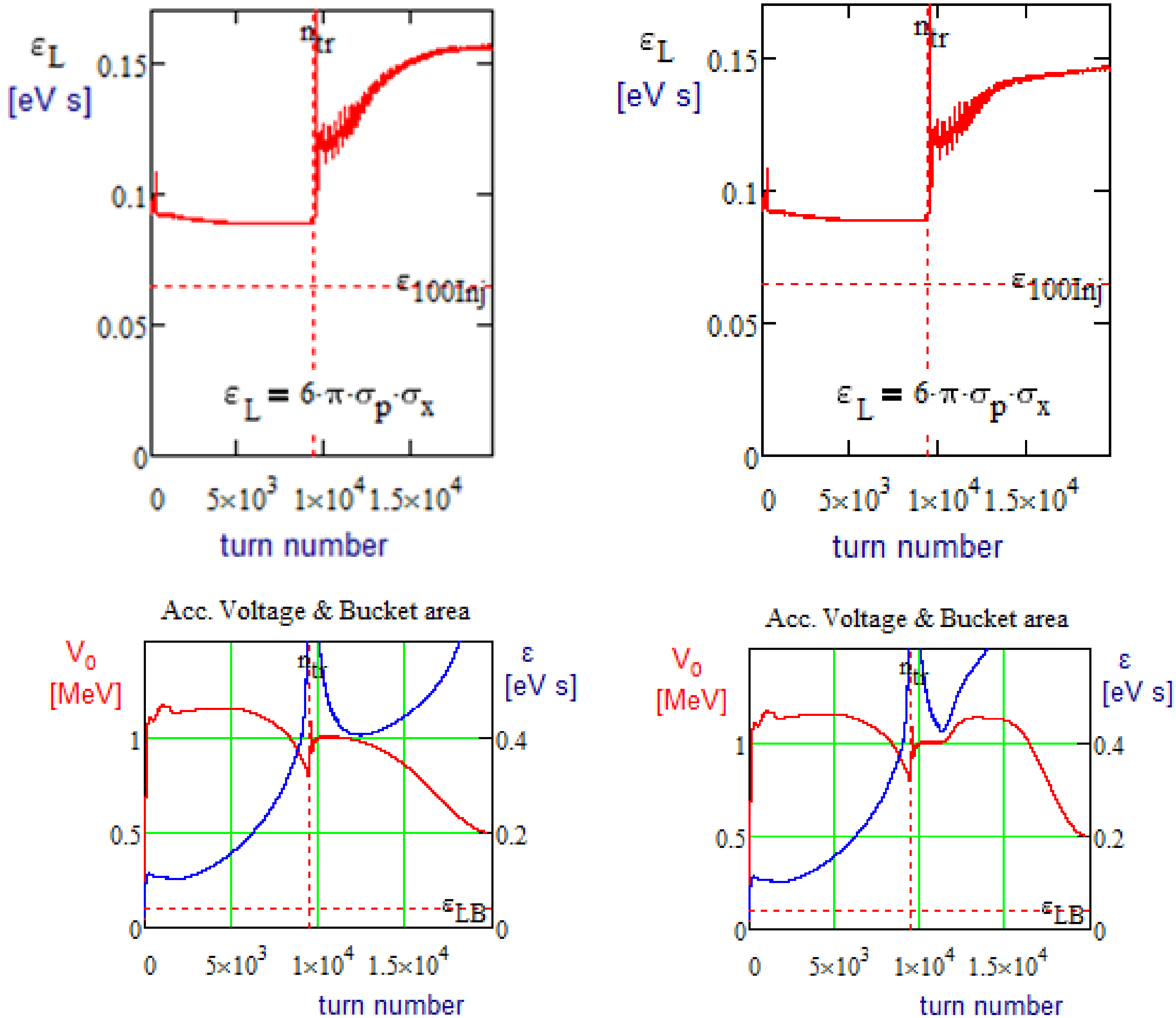

Simulation of Emittance growth for the present RF wave-form (left) and for the RF wave form with increased voltage after transition (right), Np=4.8·10¹² (15 turn inj.)

Beam Phase Space Dynamics near Transition

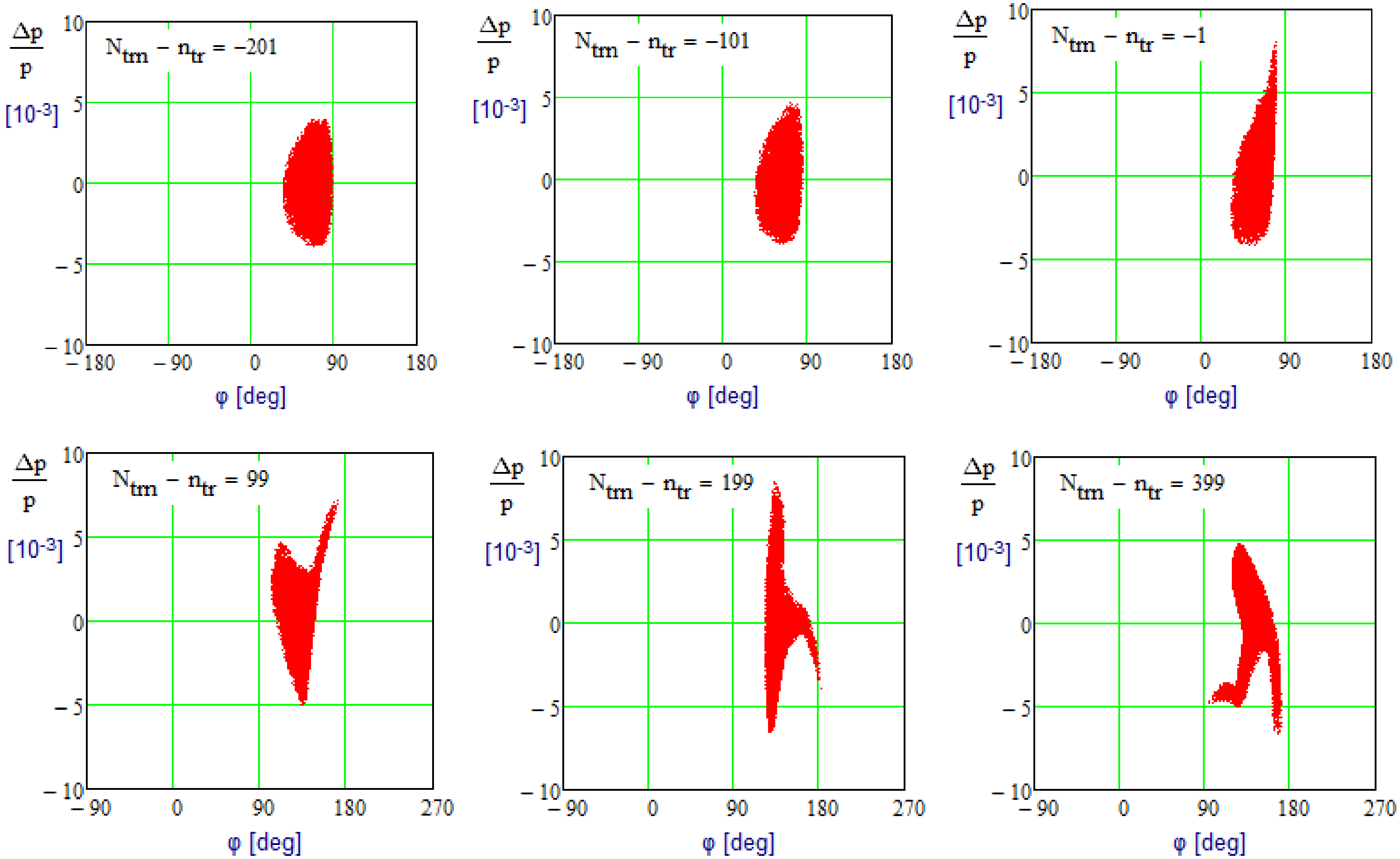

- Synchrotron motion is lost for about 150 turns
  - ⇨ Relative momentum droop between bunch center and tails is $\Delta p/p \approx (150 * 300\ \mathrm{kV})/(5\ \mathrm{GeV}) \approx 0.009$
- Effect of impedance cannot be compensated by RF voltage manipulation
  - ♦ 2nd harmonic can only help due to overall voltage increase

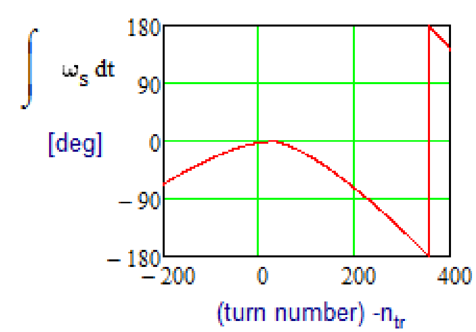

Q-jump versus Gamma-t Jump

- γ-jump is a well-tested technique to mitigate problems due to $Z_{||}$
- Two possibilities: (1) γ-jump when Q stays constant; and (2) Q-jump
  - At minimum, $\Delta\alpha \sim \pm 3\cdot 10^{-4}$ (±1%) is required to make the jump useful
- Q-jump is achieved by ramping all trim quads in S-straights

  ⇨ ΔI_Q=4.27 A, Δ(GdL)=106 G, ΔQ_x=0.039, $\Delta\alpha$=$3.15\cdot 10^{-4}$

  Tune changes within ±0.1 look acceptable => $\Delta\alpha_{max}=\pm 8.1\cdot 10^{-4}$
- Formally γ_t- jump looks as more promising technique
  - However Booster has non-zero dispersion

  ⇨In the first order, α cannot be changed without affecting tune.
  - But it can be done in the second order
  - To make it effective the resonant excitation of dispersion was suggested (L. C. Teng, 1970):

$$\gamma_t^2 = \frac{2\pi R}{\delta L} \cong \nu^2 - \frac{9}{8}\frac{a^2}{R^2}\frac{\nu^4}{\nu^2 - n^2}$$

  - To achieve the same change in α the 6-th harmonic requires ~30% higher quad current change than the 7th harmonic
    - but makes smaller dispersion excitation

      $\Rightarrow$ 6th is the preferred choice

Gamma-t Jump

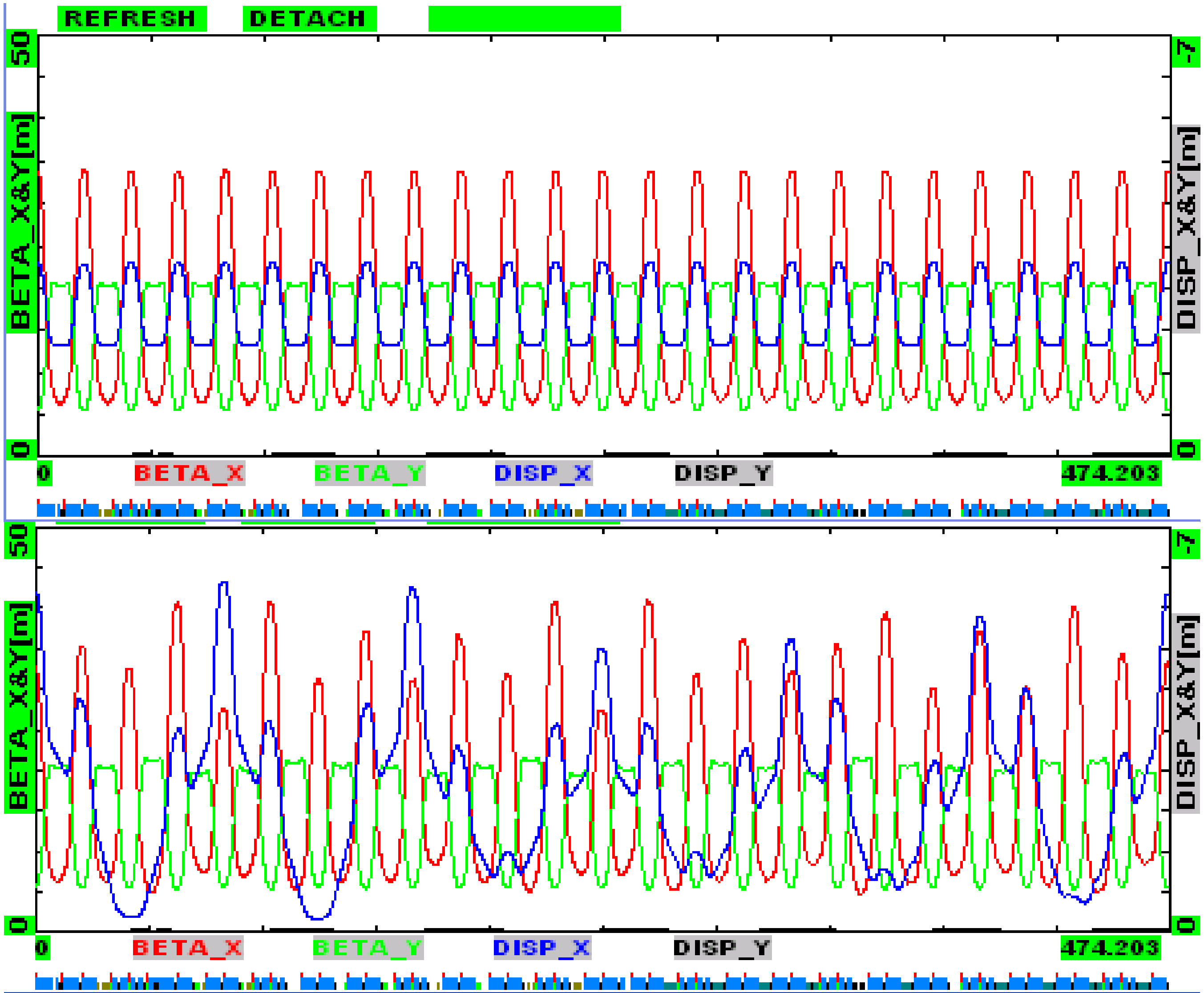

- Peak quad current of 58 A is required to achieve $\Delta\alpha=1.6\cdot10^{-4}$
  - It results in twice larger peak dispersion and half of momentum aperture
  - It also requires ~5 times larger current change in quads
- γ_t-jump does not look competative to the Q-jump

Q-jump with Present Trim Quads

- Trim quad specifications determine:
  - $d(GdL)/dt|_{max}=0.88$ kG/ms
  - $dI/dt|_{max}=35.6$ A/ms
  - That requires peak voltage of 78 V
- Maximum power supply voltage is 160 V
  - ⇨ twice larger ramp rate looks possible
- Skin-effect does not limit the field ramp rate

$$\frac{dG}{dt}+\frac{G}{\tau}=\frac{G_0(t)}{\tau}, \quad \tau=\frac{\pi\sigma a d}{c^2}\equiv\frac{ad}{2\delta^2}$$

Vacuum chamber parameters:

a = 66 mm, d = 1.6 mm,

σ^{-1} = 74 μΩ/cm (stainless steel)

⇨ τ = 45 μs.

- Such value makes negligible effect on quad gradient inside the vacuum chamber

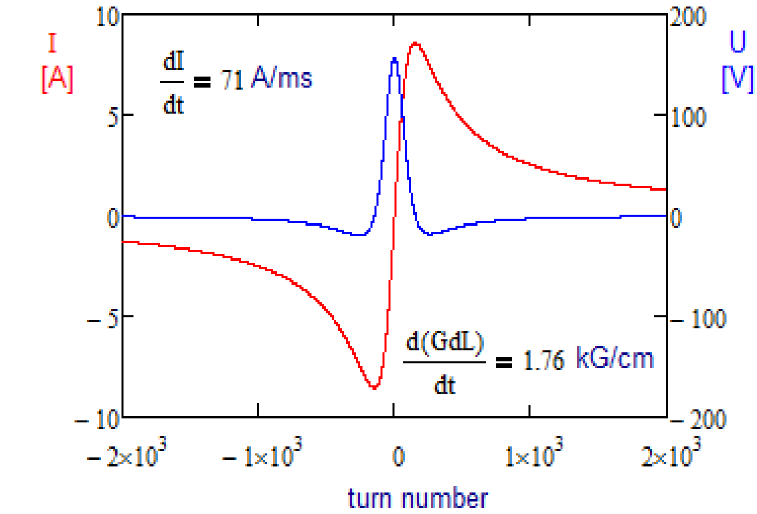

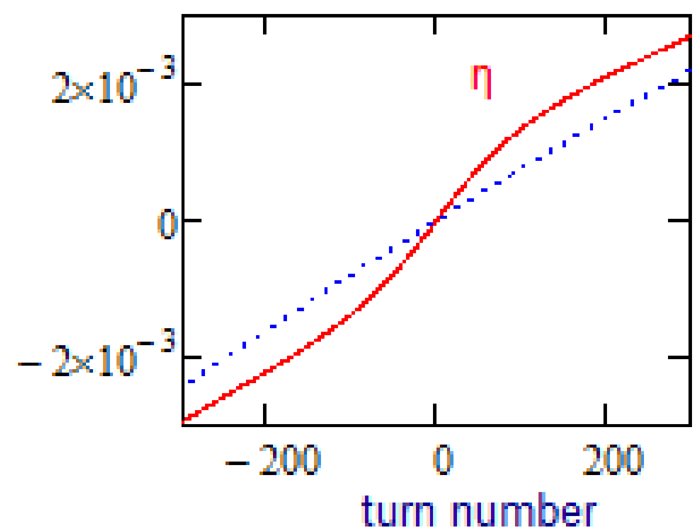

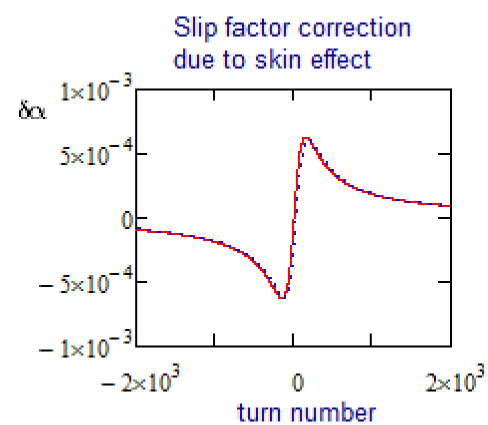

Transition Crossing with Q-jump

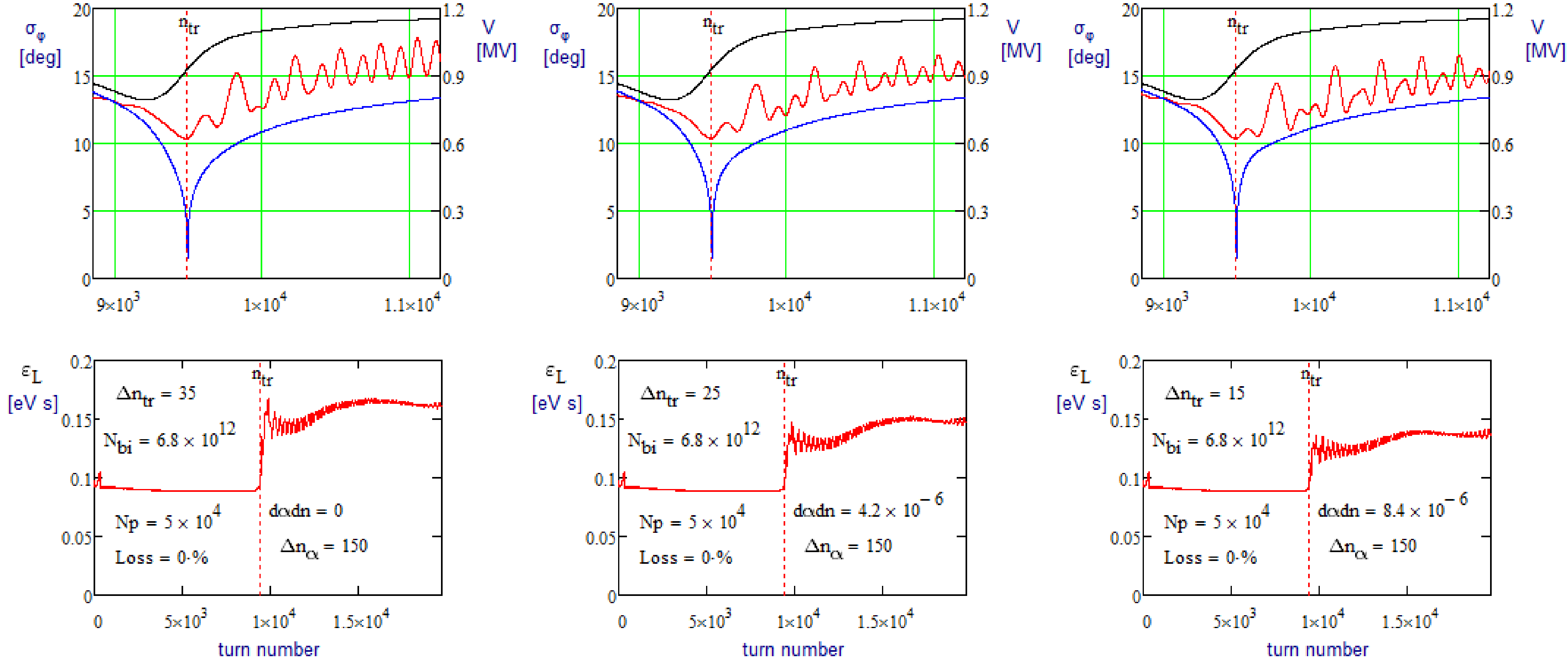

No Q-jump

Soft Q-jump:
ΔQ=±0.04
Δα=±3.15·10^{-4}
dI/dt$_{max}$=35.4 *A/ms*
ΔI$_{max}$=4.28 *A*
V$_{max}$=78 V

Normal Q-jump:
ΔQ=±0.079
Δα=±6.3·10^{-4}
dI/dt$_{max}$=70.8 *A/ms*
ΔI$_{max}$=8.55 *A*
V$_{max}$=155 V

$$\Delta\alpha(n) = \frac{d\alpha}{dn}\frac{\Delta n_\alpha{}^2 n}{\Delta n_\alpha{}^2 + n^2}$$

Negative Mass Instability

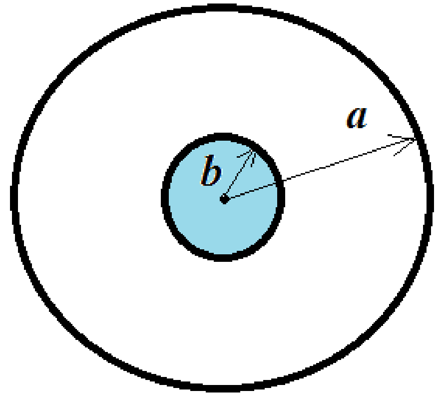

- Space charge impedance at high ω (round vac. chamber and beam, a=2.5 cm, a/b=2.3):

$$\frac{Z_n}{n} = -\frac{iZ_0}{2\pi\gamma^2\beta}\frac{1}{b^2k^2}\left(1-\frac{I_0(ka)K_1(kb)+I_1(kb)K_0(ka)}{I_0(ka)\left(I_0(kb)K_1(kb)+I_1(kb)K_0(kb)\right)}\right), \quad k=\frac{2\pi n}{\gamma C}$$

$$\frac{Z_n}{n} \approx -\frac{iZ_0}{\gamma^2\beta}\begin{cases}\ln\left(a/b\right)+1/2\,, & ka \ll 1\\ 2/k^2b^2\,, & kb \gg 1\end{cases}$$

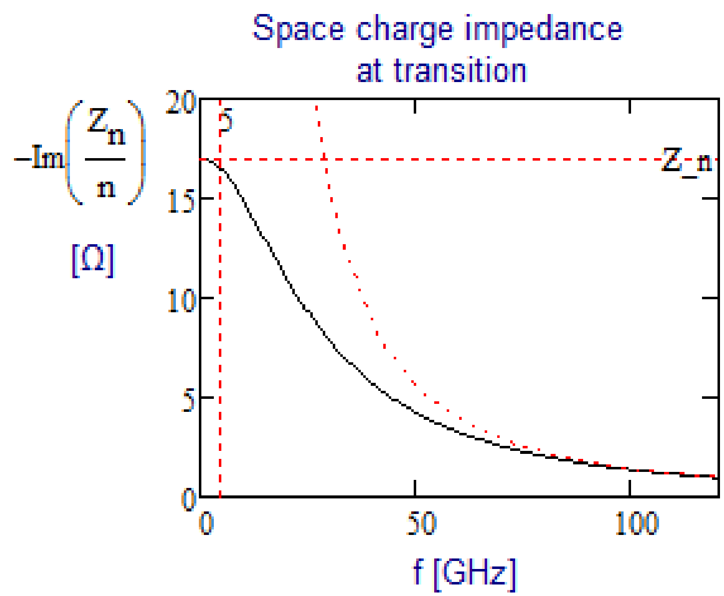

- The instability threshold is determined by low frequencies (ω<<5 GHz)

$$\eta > \eta_b \equiv \frac{eI_{peak}\left|\mathrm{Im}\left(Z_n/n\right)\right|}{2\pi mc^2\beta^2\gamma\sigma_p{}^2}$$

In the absence of 2nd order slip-factor the beam is formally unstable for about first 85 turns after transition

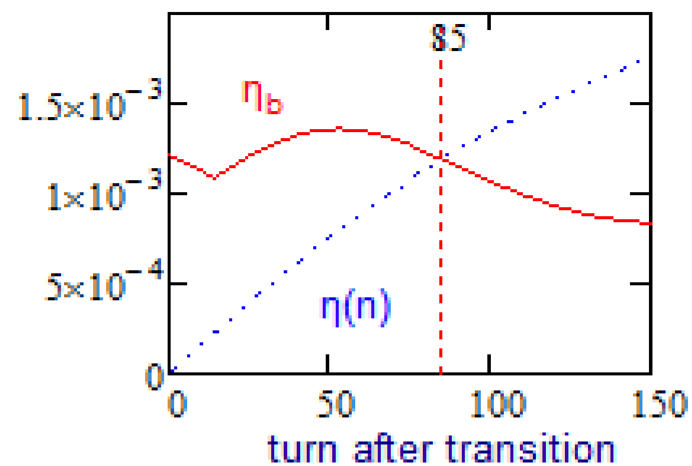

- Two questions
  - How fast instability?
  - Can it be stabilized by the second order slip-factor?

Negative Mass Instability (2)

- If the system is well above the instability threshold the hydrodynamic model can be used
  - The growth rate per turn for *n*-th harmonic is:

$$\lambda_{d_n} \equiv \frac{\lambda_n}{f_0} = n\sqrt{\frac{2\pi e I_{peak}\left|\mathrm{Im}\left(Z_n / n\right)\right|\eta}{mc^2\beta^2\gamma\sigma_p{}^2}}$$

  - At high frequency end the growth time is a few turns and the instability has to be stabilized by other mechanisms

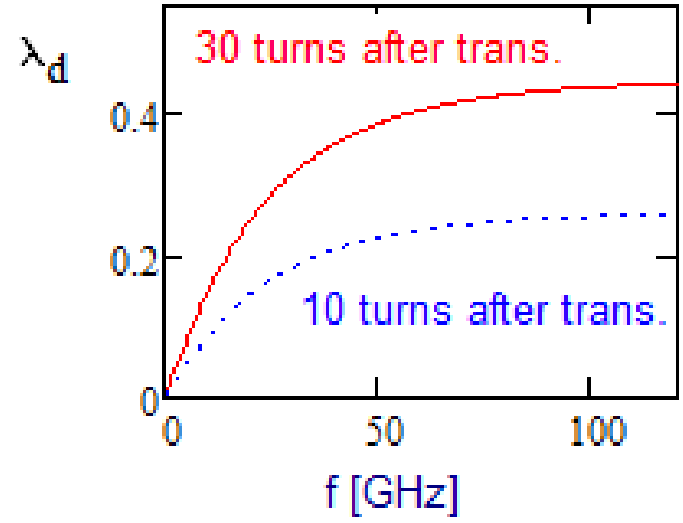

- Second order slip factor

$$\delta\omega = \omega_0\left(\eta\frac{\Delta p}{p} + \eta_p\left(\frac{\Delta p}{p}\right)^2 + \ldots\right)$$

  - Corresponding rms frequency spread for Gaussian distribution ($\sigma_p \equiv \sqrt{\overline{(\delta p / p)^2}}$)

$$\sigma_\omega \equiv \sqrt{\overline{\delta\omega^2}} = \omega_0\sqrt{\eta^2\sigma_p{}^2 + 3\eta_p{}^2\sigma_p{}^4}$$

⇨ An estimate for the stability threshold

$$\eta_p > \eta_{bp} \equiv \frac{e I_{peak}\left|\mathrm{Im}\left(Z_n / n\right)\right|}{2\sqrt{3}\pi mc^2\beta^2\gamma\sigma_p{}^3}$$

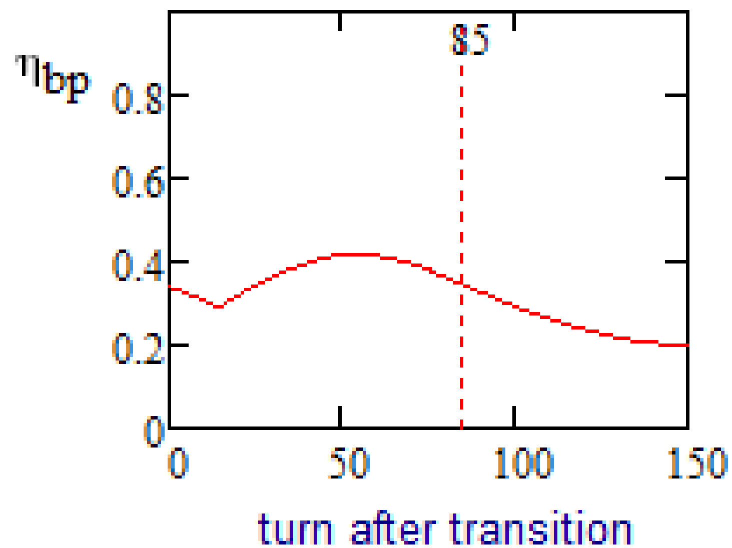

$\eta_p \geq 0.4$ is required for stabilization

Second Order Slip-factor

- Second order slip factor is closely related to chromaticity
  - Smooth lattice approximation

$$\eta_p = -\frac{1}{Q_x^{\,3}}\left(\xi + \frac{Q_x^{\,2}-1}{2Q_x}\right) + \frac{3}{2}\frac{\beta^2}{\gamma^2} \xrightarrow[\text{transition}]{\text{Booster at}} \frac{\xi}{300} + \frac{1}{35}$$

    predicts quite small value
  - MAD does not make trustable answer
  - Additional investigations are going on

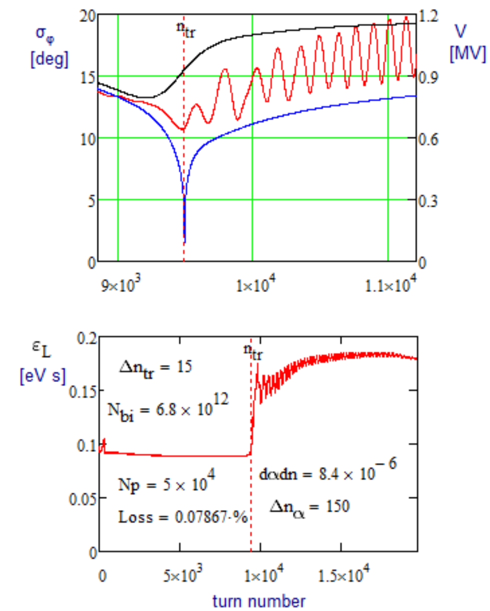

α_p=0.1

- Simulations show high sensitivity of transition crossing to η_p

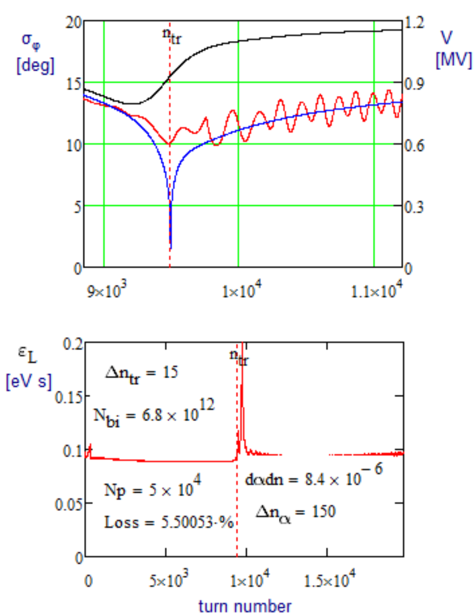

α_p=-0.3

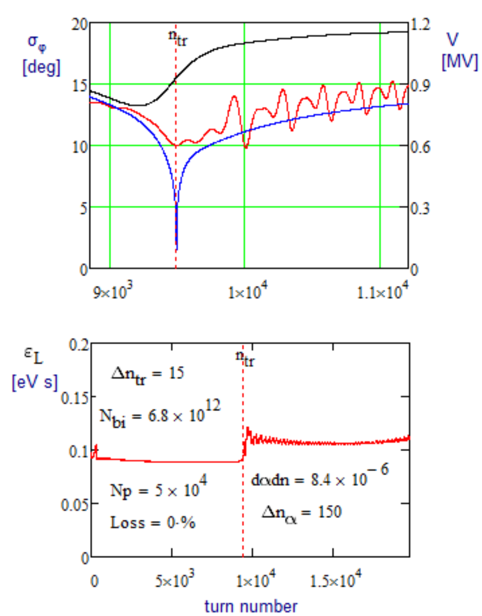

α_p=-0.2

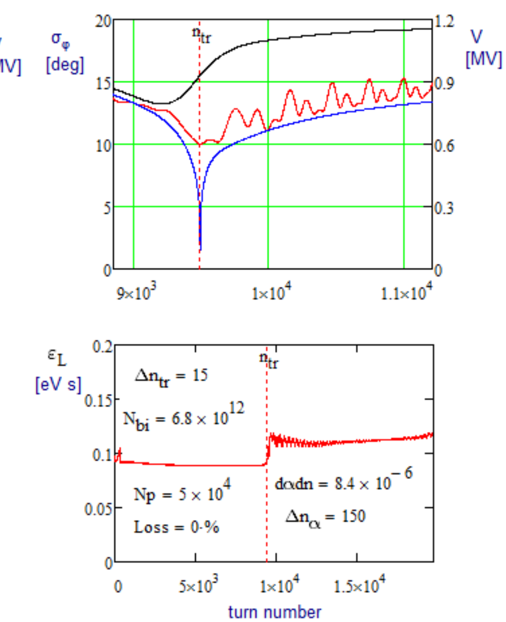

α_p=-0.1

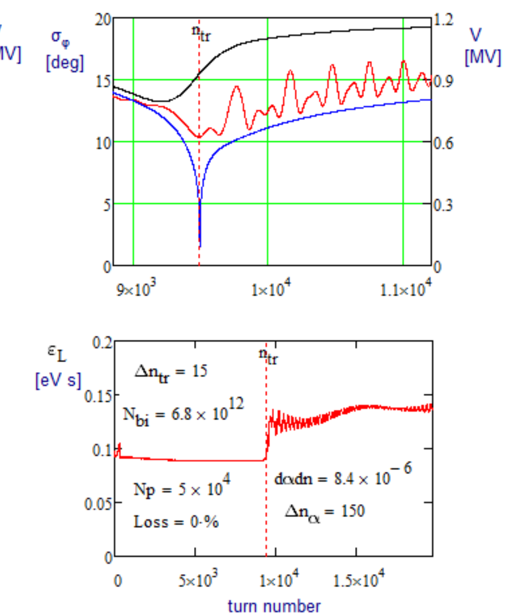

α_p=0

Conclusions

- Measurements and simulations showed transition crossing details which were not known before
  - There are a lot of features in instrumentation which need to be accounted of fixed
    - Separate discussion is required
- Simulations show that the transition crossing at PIP-II intensity without additional growth of longitudinal emittance is possible
  - 1.2 MV RF voltage is required
  - Q-jump at transition with present trim quadrupoles is greatly helpful
  - 20 Hz ramp rate will result in faster transition and, consequently, will result in additional decrease of emittance growth
- Effects of negative mass instability require better understanding
- Second order slip-factor is important factor and requires better understanding both theoretically and experimentally